QCD in DIS at HERA

Gregorio Bernardi
LPNHE - Paris

on behalf of the

H1 and ZEUS Collaborations

SLAC - Topical Conference, 12^{th} of August 1998

Many thanks to my H1 and ZEUS colleagues, in particular to Ursula Bassler, for the preparation of this talk.

Outlay

- F_2 at Low and Intermediate Q^2

→ transition region with photoproduction $Q^2 \to 0$
→ F_2 in Next to Leading Order and DGLAP evolution
→ determination of F_L
→ extraction of $F_2^{c\bar{c}}$
→ measurements of the gluon density $xg(x, Q^2)$

- Jets

→ the gluon density from jets
→ jet shapes in DIS
→ measurement of α_S:
  from integrated jet rates
  from differential jet rates
  from event shape variables

- Cross-Sections at High Q^2

→ influence of xF_3 and Z° exchange
→ Neutral Current cross-sections, high x
→ Charged Current cross-sections, W-mass
→ NC/CC ⇒ ratio u/d quark densities

DIS Events at HERA

Low Q^2, low x event

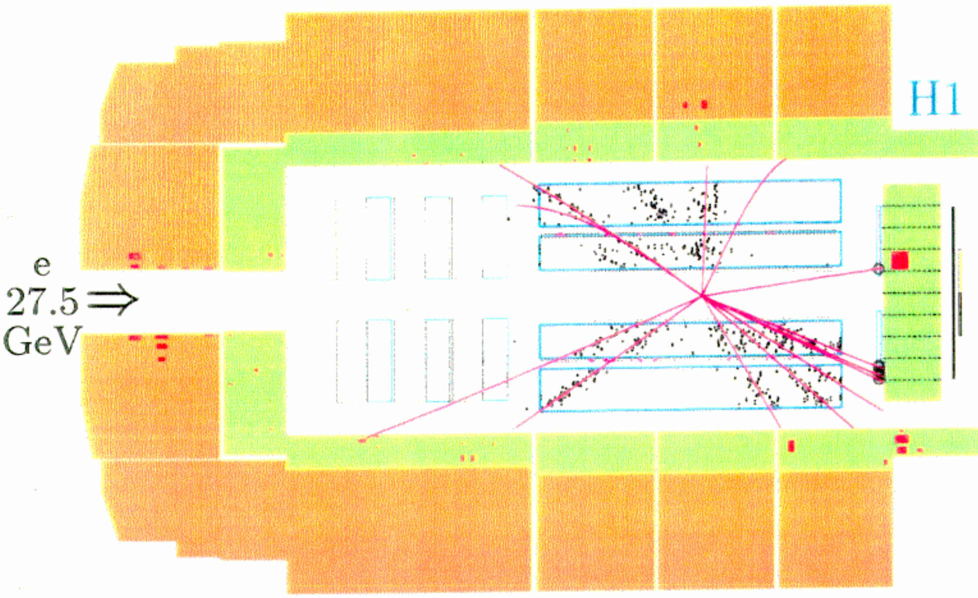

measured quantities:

e^+: energy E

polar angle θ

hadrons: $\Sigma = \sum_h (E_h - p_{z,h})$

$p_{T,h} = \sum_h p_{t,h}$

$\tan \gamma/2 = \Sigma / p_{T,h}$

Di-jet event

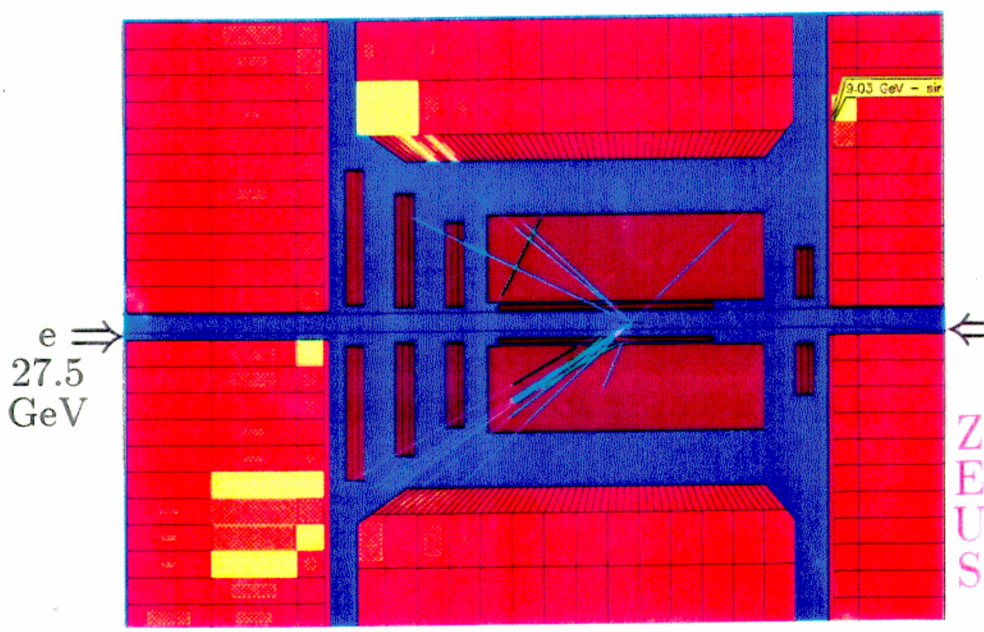

Deep Inelastic Scattering at HERA

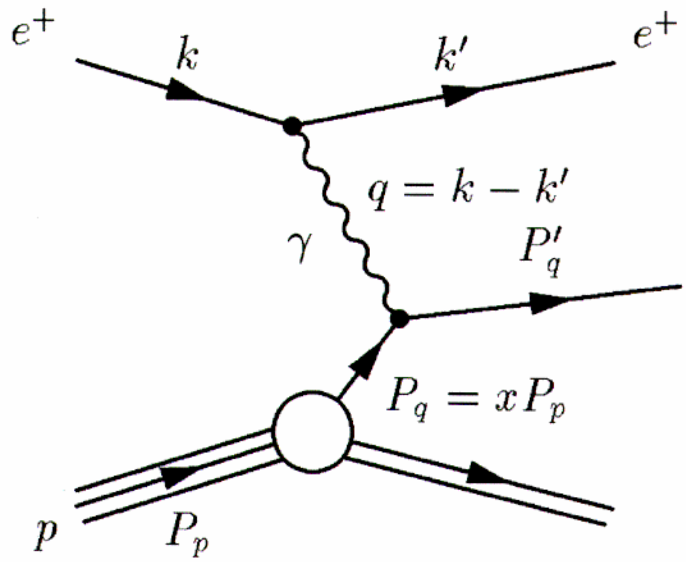

$Q^2 = -q^2 = -(k - k')^2$
4-momentum transfer

$x = Q^2/(2p \cdot q)$
parton momentum fraction

$y = p \cdot q/(p \cdot k)$
fractional energy transfer

$W^2 = (p+q)^2 \approx Q^2/x$
mass^2 of hadronic system

Structure Function F_2 in Quark Parton Model:

$$\frac{d^2\sigma^{e^\pm p}}{dxdQ^2} = \frac{2\pi\alpha^2}{Q^4x}\,[1+(1-y)^2]\,F_2(x,Q^2)\,\cdot(1+\delta_{QED})$$

Related to the parton densities:

$$F_2(x) = x\sum_{i=1}^{n_f} e_i^2(q_i(x) + \overline{q}_i(x))$$

Longitudinal Structure Function: $F_L = 0$ in QPM
(Callan-Gross relation)

δ_{QED} : QED radiative corrections are precisely known ($\simeq 1\%$) and are corrected for

Kinematics and Measurement

Methods used for Kinematic Reconstruction:

- **Electron Method:** $y_e = 1 - \frac{E'_e}{E_e}\sin^2\frac{\theta_e}{2}$ $Q_e^2 = 4E'_eE_e\cos^2\frac{\theta_e}{2}$
  most precise at low x but very sensitive to QED radiation
  poor x resolution at low y, but good Q^2 resolution in full range

- **Σ Method:** $y_\Sigma = \frac{\Sigma}{\Sigma + E'_e(1-\cos\theta_e)}$ $Q_\Sigma^2 = \frac{E_e^2\sin^2\theta_e}{1-y_\Sigma}$
  good x resolution also at low y
  independent of QED initial state radiation

- **$e\Sigma$ Method:** $x_{e\Sigma} = x_\Sigma$ $Q_{e\Sigma}^2 = Q_e^2$
  precise over the whole kinematic range
  $\Rightarrow$ extension of the measurement at high x

- **Double Angle Method:** x_{DA}, Q_{DA}^2 from θ_e, γ_h
  high precision at high Q^2, but sensitive to QED radiation
  independent of energy scale $\Rightarrow$ used for calibration

- **Hadron Method:** $y_h = \frac{\Sigma}{2E_e}$ $Q_h^2 = \frac{p_{T,h}^2}{1-y_h}$
  low precision, but only method for charged current

Measurement:

- (x, Q^2) binning: 5 bins/order of magnitude in x
  8 bins/order of magnitude in Q^2
- Purity and Stability of the (x, Q^2) bins $\geq 30\%$
- Background Subtraction (Photoproduction)
- Luminosity known within $1.5 - 2.5\%$ at HERA
- QED radiative corrections applied
  $\Rightarrow \left.\frac{d^2\sigma}{dx\,dQ^2}\right|_{Born}$ measured at fixed x, Q^2
  after bin center correction

F_2 Results at HERA '94

1994: $\mathcal{L} \sim 3\ \text{pb}^{-1}$

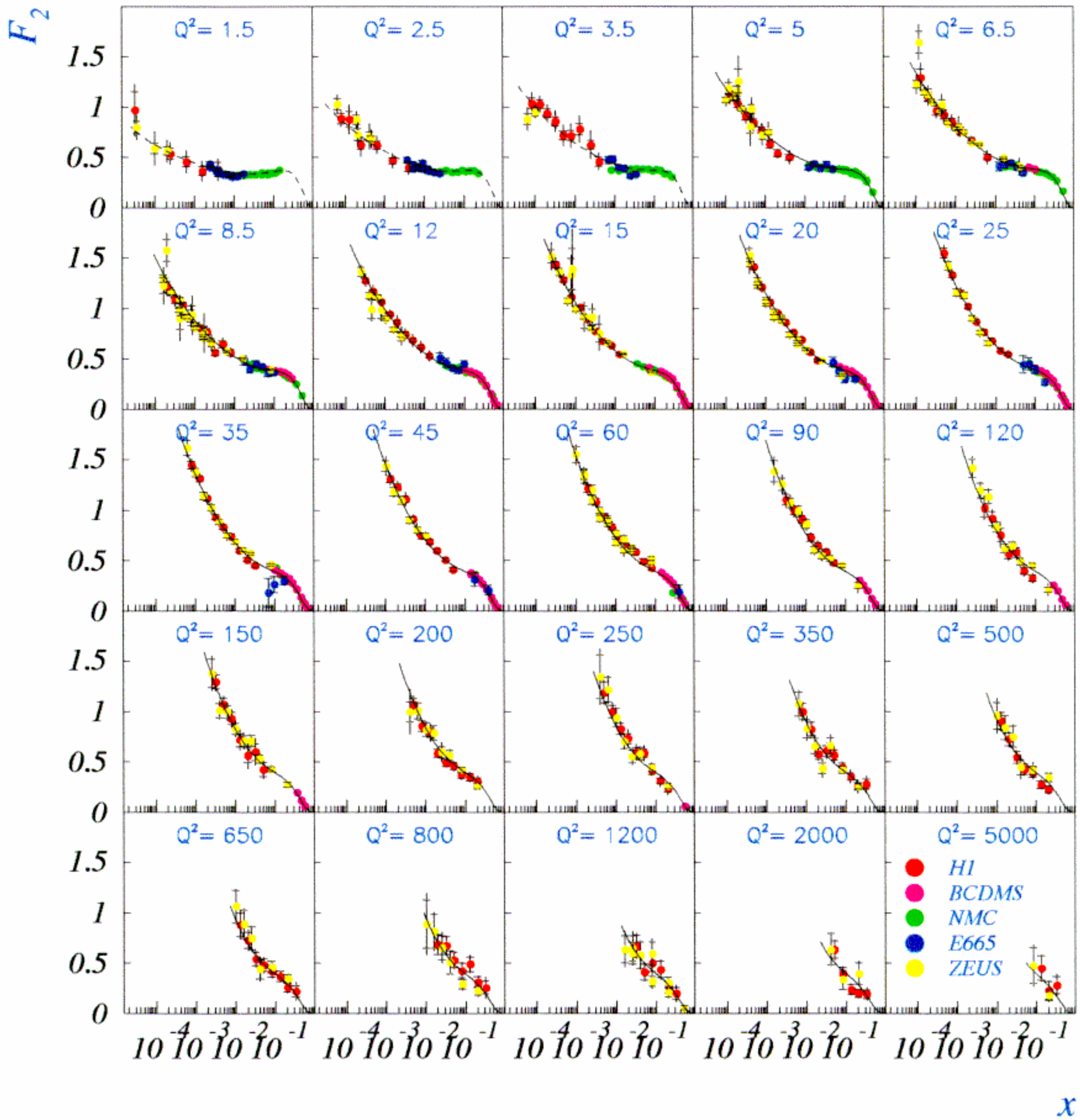

- Strong rise of $F_2(x, Q^2)$ at low x for a fixed Q^2
- Good agreement between HERA and fixed target exp.
- NLO QCD (DGLAP) fit gives good description down to $Q^2 = 1.5\ \text{GeV}^2$
- Systematic errors $\sim 5\%$ dominant, except at high Q^2

Inclusive Measurements in (x, Q^2)

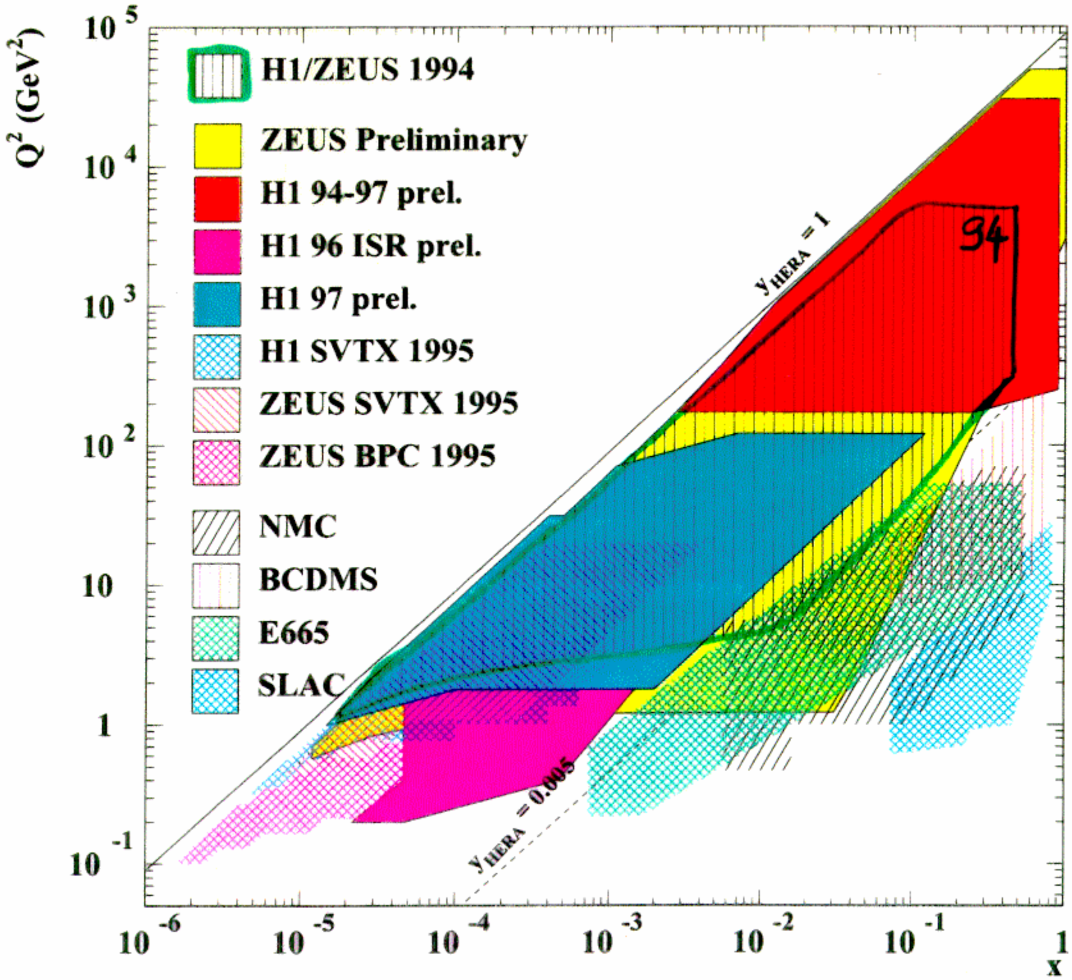

H1+ZEUS: Major extension of the kinematic range

- $x \rightarrow < 10^{-5}$: test low x limit of pQCD
- $x \rightarrow 0.65$: probe valence quark region
- $y \rightarrow 0.005$: overlap with fixed target experiments
- $y \rightarrow 0.82$: sensitivity to F_L
- $Q^2 \rightarrow 0.1$ GeV^2 : transition to γp
- $Q^2 \rightarrow 30000$ GeV^2: sensitivity to electro-weak effects

Access to the low $\boldsymbol{Q^2}$ region

$Q^2 = 4E'_e E_e \cos(\frac{\theta_e}{2})$

1. shift of the interaction point $\quad Q^2 \rightarrow 0.35\ \mathrm{GeV}^2$

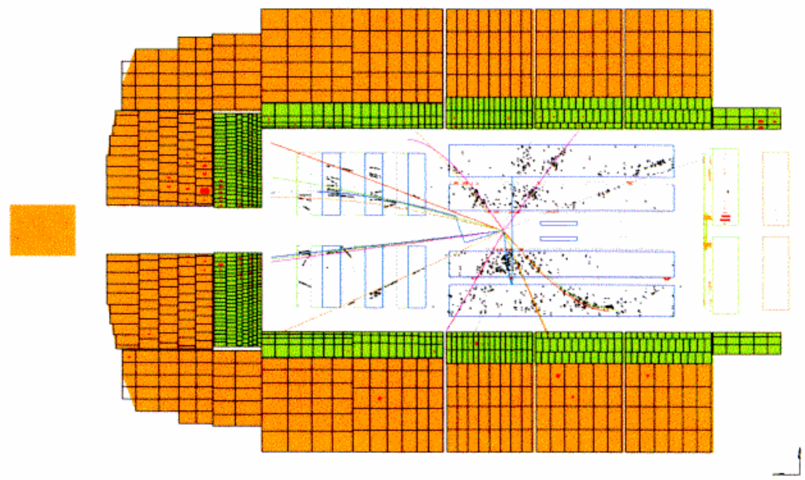

2. low angle detectors $\quad Q^2 \rightarrow 0.1\ \mathrm{GeV}^2$

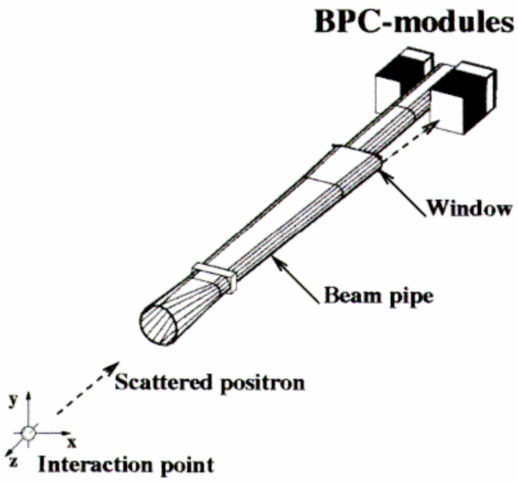

ZEUS: BPC (1995)
H1: VLQ (1998)

3. radiative events
$Q^2 \rightarrow 0.2\ \mathrm{GeV}^2$
higher x

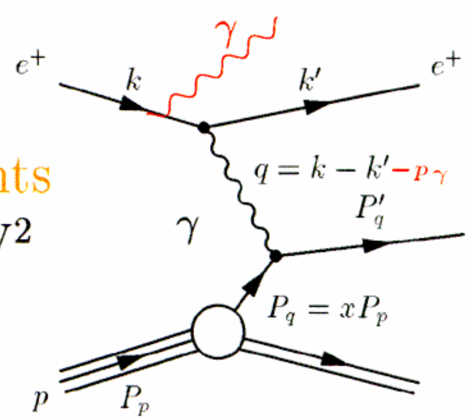

Cross-Sections at low Q^2

Define total $\gamma^* p$ cross section:

$$\sigma_{tot}^{\gamma^* p}(W^2, Q^2) = \sigma_L^{\gamma^* p} + \sigma_T^{\gamma^* p} \simeq \frac{4\pi\alpha^2}{Q^2} F_2$$

$$W^2 \approx Q^2/x \quad \text{at low } x$$

$\Rightarrow$ comparison with γp data

- precise data from ZEUS and H1 on $\sigma^{\gamma p}$ ($Q^2 \approx 0$) and $\sigma^{\gamma^* p}$ at low Q^2 ($\approx 0.1 - 5$ GeV^2)
- 2 paradigms:
  - pQCD at very low Q_0^2 as in the GRV model, in which the DGLAP evolution starts with valence-like partons at $Q_0^2 \sim 0.4$ GeV^2
  - Regge approach as in the Donnachie-Landshoff model in which $\sigma_{tot} \propto W^{2\alpha_P}$, α_P is Q^2 independent and determined from hadron data ('soft Pomeron')
- interplay of pQCD $\leftrightarrow$ Regge phenomenology ?

How does the transition take place?

Transition when $Q^2 \to 0$

$\sigma_{\gamma^* p}(W, Q^2)$ at fixed W as function of Q^2:

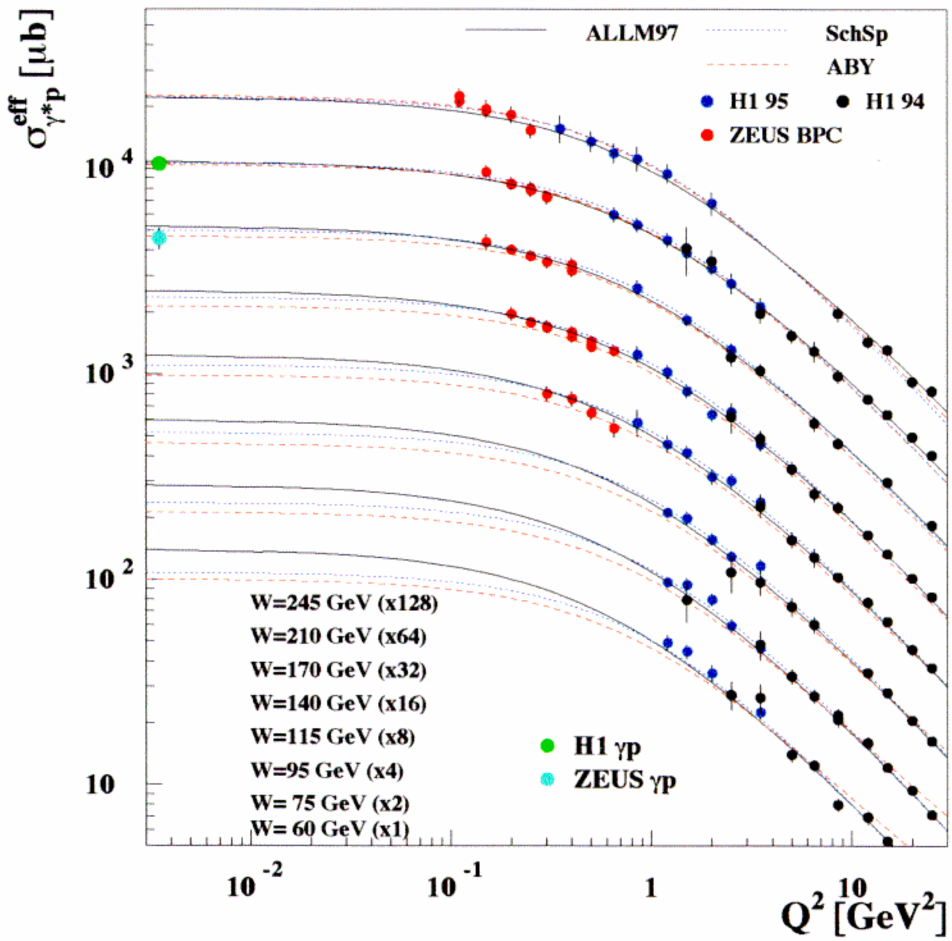

- Smooth transition to photoproduction $\sigma_{\gamma p}$ ● ●
- Constant Cross-Section up to $Q^2 \simeq 0.1$ GeV^2
- Change of behaviour $Q^2 \simeq 0.1 - 1$ GeV^2
- Fast decrease in the pert. QCD regime $Q^2 \gtrsim 1$ GeV^2
- ABY, SchSp and ALLM97 (all are fits to HERA data)
  $\Rightarrow$ good description in transition region,
  BUT no real theory
- New Measurements at $Q^2 \lesssim 0.1$ GeV^2 foreseen at HERA

Models for Transition DIS $\rightarrow \gamma p$

- at high Q^2 perturbative QCD (i.e. GRV model) describes the data
- at $Q^2 = 0$ the Regge approach (i.e. DL) is valid

How can we model the transition region ?

- Badelek and Kwiecinski (BK)
  ρ, ω, f from VDM plus
  pQCD above Q^2 matching value
- Schildknecht and Spiesberger (ScSp)
  Generalised VDM-model for
  $0<x<0.05$, $0<Q^2<350$ GeV^2 and $W>30$ GeV
- Capella et al (CKMT)
  Regge like, but with Q^2 dependent α_P
- Abramowicz et al (ALLM):
  Regge + QCD inspired parametrisation
  for all x and Q^2
- Adel, Barreiro and Yndurain (ABY)
  soft + hard input $a+bx^{-\lambda}$ at a low input scale
  each with its own NLO QCD evolution

Comparison to Photoproduction $Q^2 \approx 0$

Check the different models over the full W range in γp:

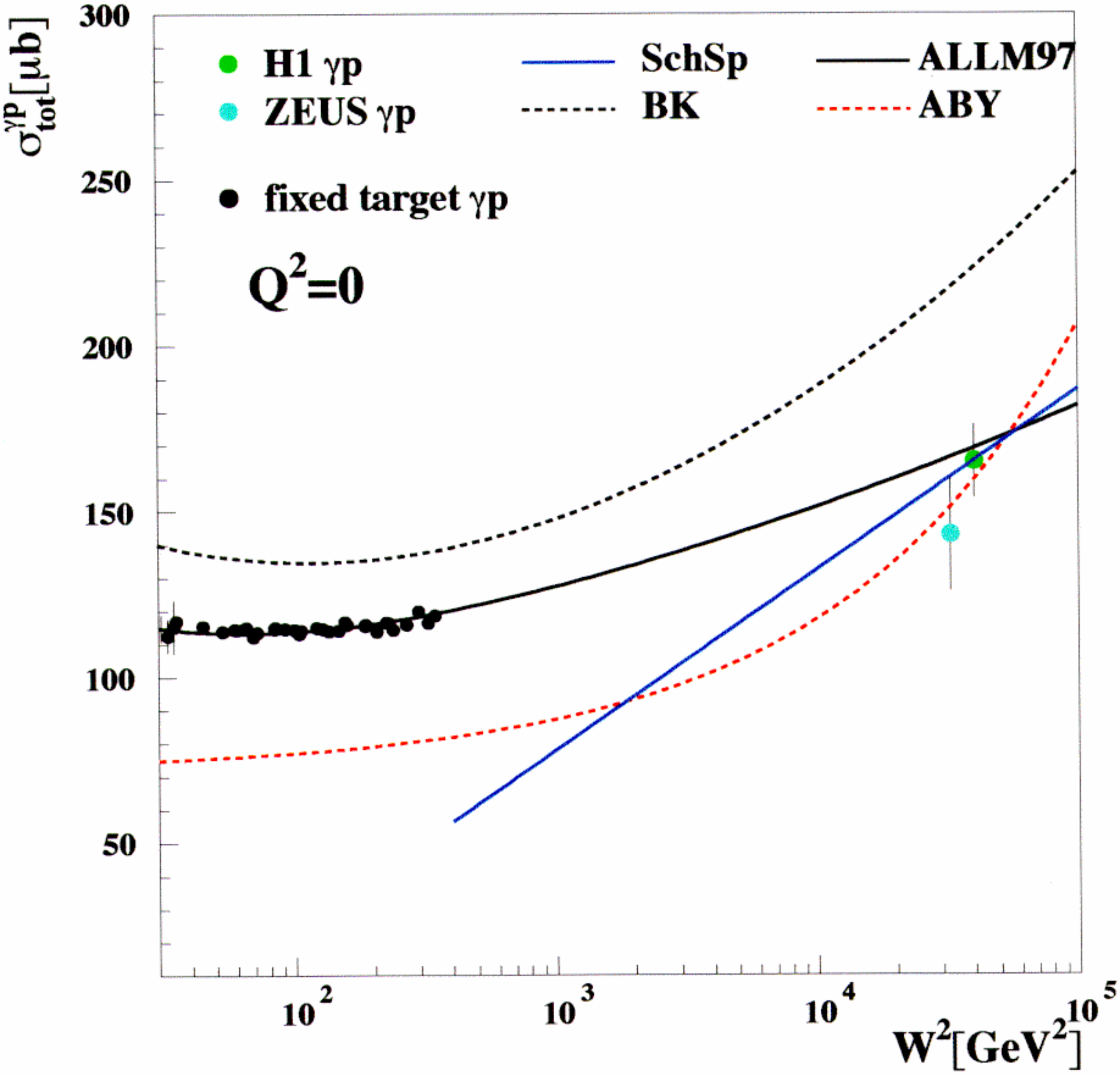

- only recent ALLM97 parametrization reproduces DIS and γp cross section over full W range
- ABY, SchSp and BK have wrong W dependence

Comparison to Photoproduction $Q^2 \approx 0$

ZEUS 1995 Preliminary

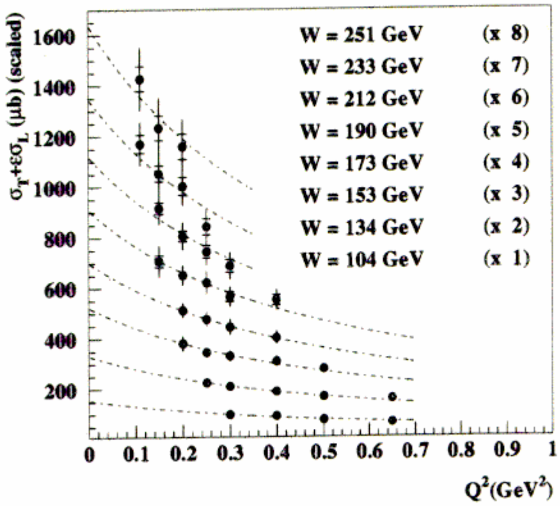

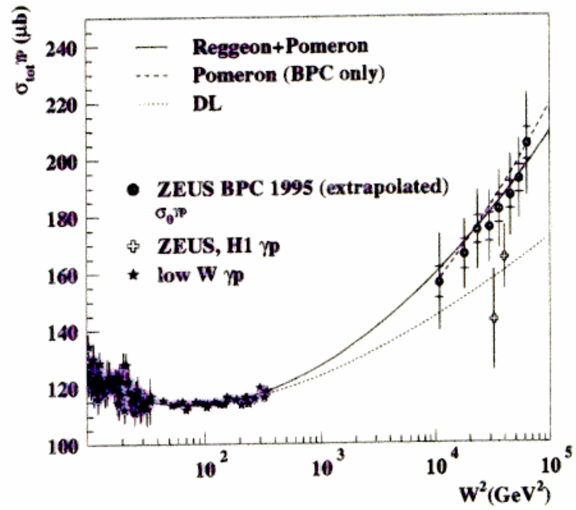

simplified GVMD ansatz:

$$F_2 = \frac{Q^2 M_0^2}{M_0^2 + Q^2} \frac{\sigma_0^{\gamma p}}{4\pi^2\alpha}$$

$$\sigma_T(W^2, Q^2) = \frac{M_0^2}{M_0^2+Q^2}\,\sigma_0^{\gamma p}(W^2)$$

$$\sigma_{tot}^{\gamma p}(W^2) = A_R (W^2)^{\alpha_R - 1} + A_P (W^2)^{\alpha_P - 1}$$

- GVDM fit to the BPC data allows extrapolation of the BPC points towards $Q^2 \simeq 0$
- Pomeron (and Reggeon) contributions must be considered to describe correctly the BPC data and real γp data, $W^2 > 3$ GeV

$\alpha_{IP} = 1.010 \pm 0.002$

$F_2(x, Q^2)$ at low Q^2

- F_2 still rises at $Q^2 = 0.11$ GeV^2 and x=6× 10^{-6}, but less strongly
- pQCD (i.e. GRV) describes the data at $Q^2 \gtrsim 1$ GeV^2

→ transition occurs at much lower Q^2 than expected

- DL Regge Model (Soft Pomeron) too low at low x, even at very low Q^2

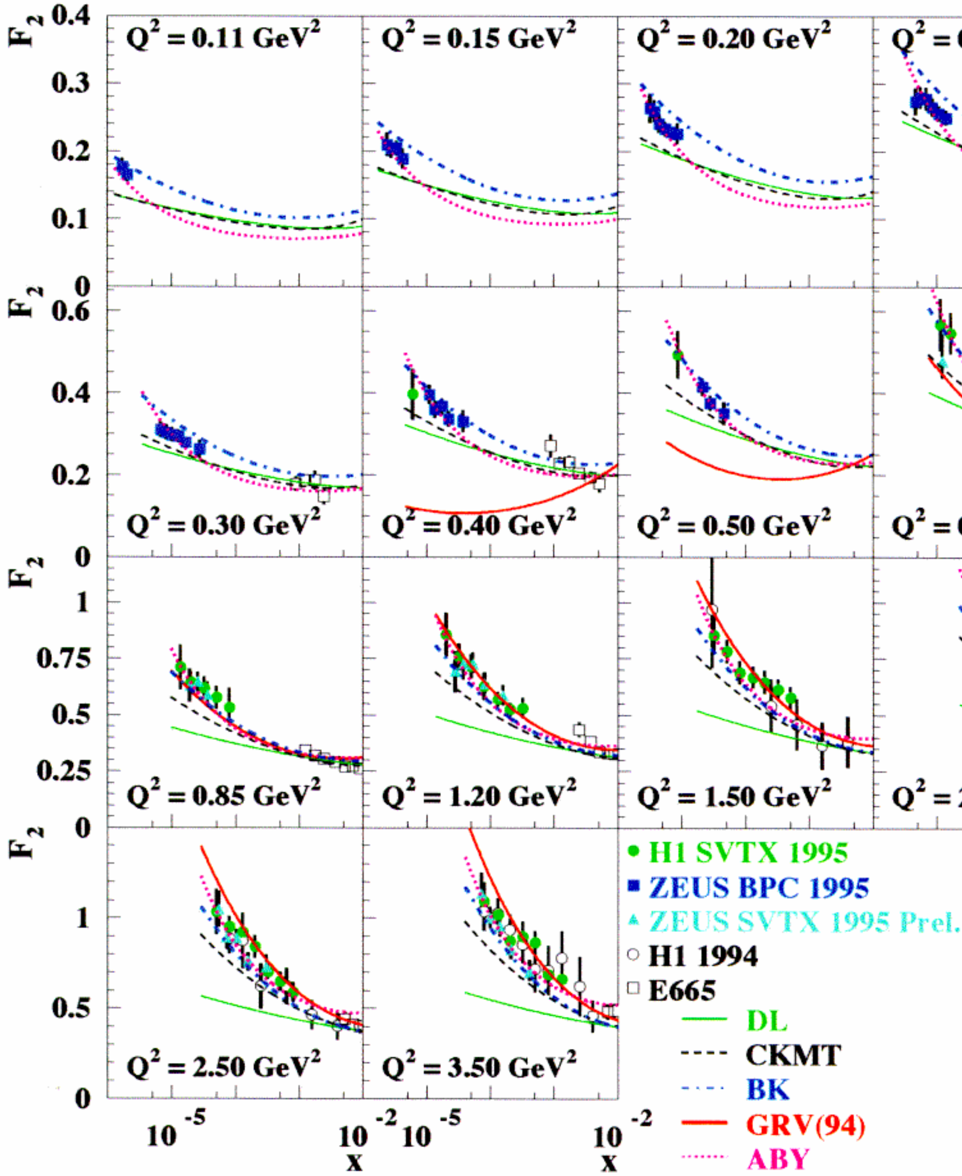

Transition Region: $x^{-\lambda}$

Fit effective x slope at fixed Q^2:

$$\lambda \approx \frac{d \ln F_2}{d \ln 1/x} \qquad \text{i.e} \qquad F_2 \propto x^{-\lambda}$$

$\Rightarrow$ precision with H1 1997 data on $\lambda \simeq 1\%(\text{stat}) \oplus 5\%(\text{syst})$

How is λ decreasing towards $\lambda = 0.08$ as expected from Soft Pomeron at $Q^2 = 0$?

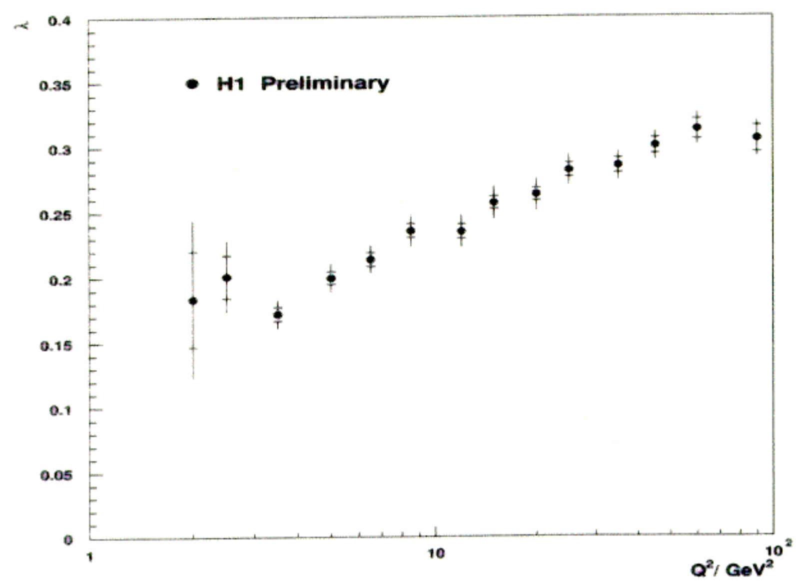

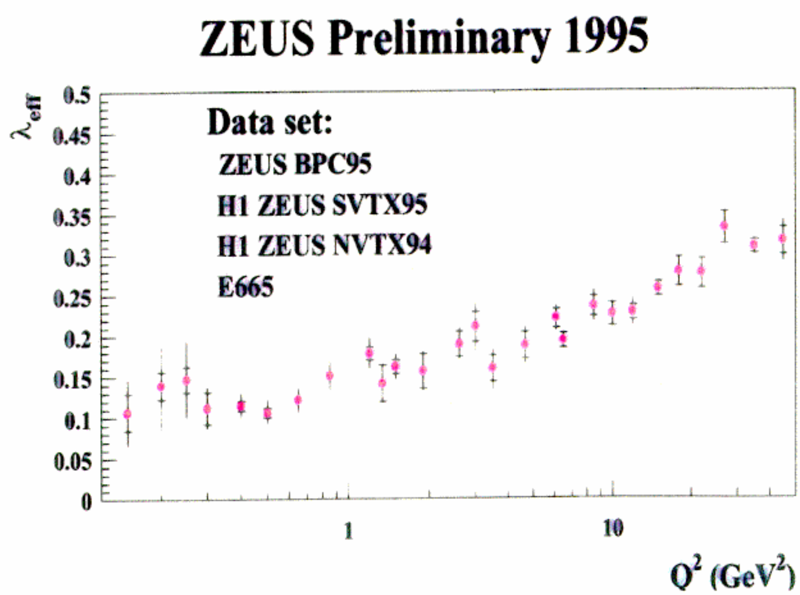

$F_2(x, Q^2)$ at Intermediate Q^2

- New high precision measurement with the 1997 data, based on $\mathcal{L} \simeq 15\ \text{pb}^{-1}$ (H1):

$\lesssim 1\%$	statistic	$2 \leq Q^2 \leq 100\ \text{GeV}^2$
$\lesssim 4\%$	systematic	

- Main error sources:
  - electron energy scale:

    $$\frac{\delta E_e}{E_e} = 0.5\%$$ based on the kinematic peak
  - hadronic energy scale:

    $$\frac{\delta E_h}{E_h} = 3\%$$ based on p_T balance $p_{T,h}/p_{T,e}$
  - electron identification: $1 - 2\%$
  - background: $< 1\%$
  - radiative corrections: 1-2%
  - tracking efficencies: 1-2 %

→ slightly bigger errors at the edge of the phase space

Precision Measurement ⇒

Test of NLO perturbative QCD

DGLAP Equations in QCD

- From QCD (schematically):

Leading Order:	$F_2(x)$	$= x \sum_{i=1}^{nf} e_i^2 (q_i + \bar{q}_i)$
NLO $\overline{\text{MS}}$:	$F_2(x, Q^2)$	$= x \sum_{i=1}^{n_f} e_i^2 C_q \otimes (q_i + \overline{q_i}) + C_g \otimes g$

- Define parton densities:

xq_{NS}	$= \sum_{i=1}^{n_f} (xq_i - x\overline{q_i}) = xu_{val} + xd_{val}$	Non Singlet
$x\Sigma$	$= \sum_{i=1}^{n_f} (xq_i + x\overline{q_i})$	Singlet
$xg(x)$		Gluon density

- DGLAP evolution of parton densities:

$$\frac{\partial}{\partial t} q_{NS}(x,t) = \frac{\alpha_s(t)}{2\pi} P_{qq}^{NS} \otimes q_{NS}(y,t); \quad t = \log \frac{Q^2}{\Lambda^2}$$

$$\frac{\partial}{\partial t} \begin{pmatrix} \Sigma(x,t) \\ g(x,t) \end{pmatrix} = \frac{\alpha_s(t)}{2\pi} \begin{pmatrix} P_{qq} & P_{qg} \\ P_{gq} & P_{gg} \end{pmatrix} \otimes \begin{pmatrix} \Sigma(y,t) \\ g(y,t) \end{pmatrix}$$

→ Splitting Functions P_{ij} known to NLO
→ Coefficient Functions $C_{q,g}$ known to NLO

⇒ DGLAP predicts Q^2 slope of $F_2(x, Q^2)$ for given parton densities at $Q^2 = Q_0^2$

No prediction on the x dependence at Q_0^2
⇒ must be obtained from a QCD fit to the data

H1 and ZEUS NLO-QCD fits

- **Fit Conditions and Assumptions:**
  - u,d,s massless partons
  - c from BGF calculated at NLO (Riemersma et al.) in $\overline{MS}$
    $m_c = 1.5$ GeV, scale $\mu^2 = Q^2 + m_c^2$
  - Full treatement of correlated systematic errors
  - Theoretical uncertainties from α_s and m_c
  - Momentum Sum rule: $\int_0^1 dx\, x(g+\Sigma) = 1$
  - Quark Counting Rules: $\int_0^1 dx\, u_v = 2$, $\int_0^1 dx\, d_v = 1$
  - Assume $\bar{u} = \bar{d}$ s= 20% of total sea at Q_0^2
  - Discard data with x > 0.5 at low Q^2
- **Input Parametrisations:**

$$xg\ (x, Q_0^2) = A_g x^{B_g}(1-x)^{C_g}(1+D_g x)$$
$$xu_v(x, Q_0^2) = A_u x^{B_u}(1-x)^{C_u}(1+D_u x + E_u\sqrt{x})$$
$$xd_v(x, Q_0^2) = A_d x^{B_d}(1-x)^{C_d}(1+D_d x + E_d\sqrt{x})$$
$$xS\ (x, Q_0^2) = A_s x^{B_s}(1-x)^{C_s}(1+D_s x + E_s\sqrt{x})$$

- **Datasets Used:**
  - ZEUS: ZEUS 94/5 data with $Q^2 > 1.5$ GeV^2
    - NMC p+d data
    - $Q_0^2 = 7$ GeV^2
    - $\alpha_s(M_Z^2)$=0.118
  - H1: H1 94+95+96/7 data with $Q^2 > 1.5$ GeV^2
    - NMC and BCDMS p+d data
    - $Q_0^2 = 1$ GeV^2
    - $\alpha_s(M_Z^2) = 0.118 \pm 0.05$
    - $D_g = 0$

F_2 and perturbative QCD

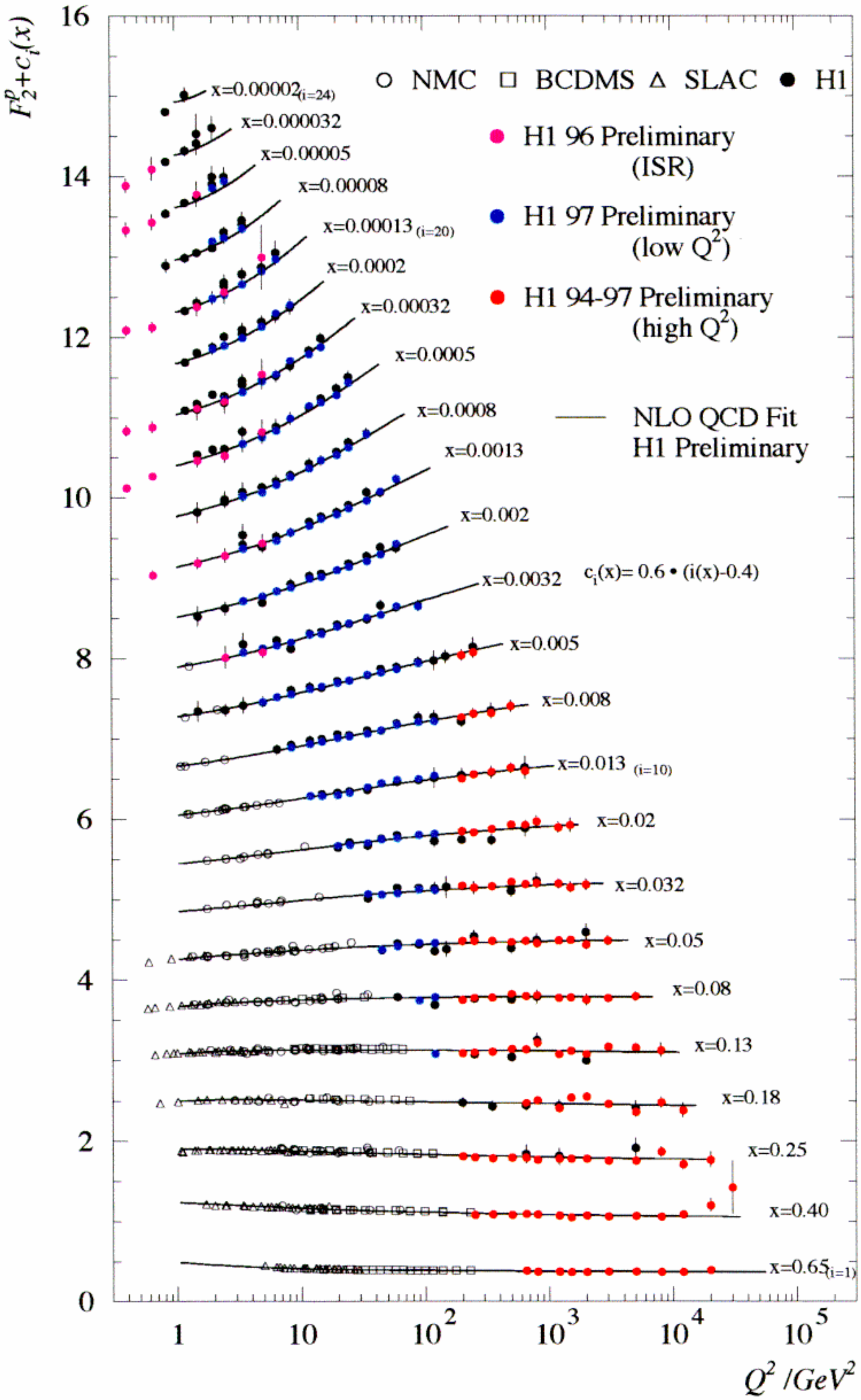

- Good description of the data by the NLO DGLAP fit over more than 4 orders of magnitude in x and Q^2

Scaling Violations of F_2

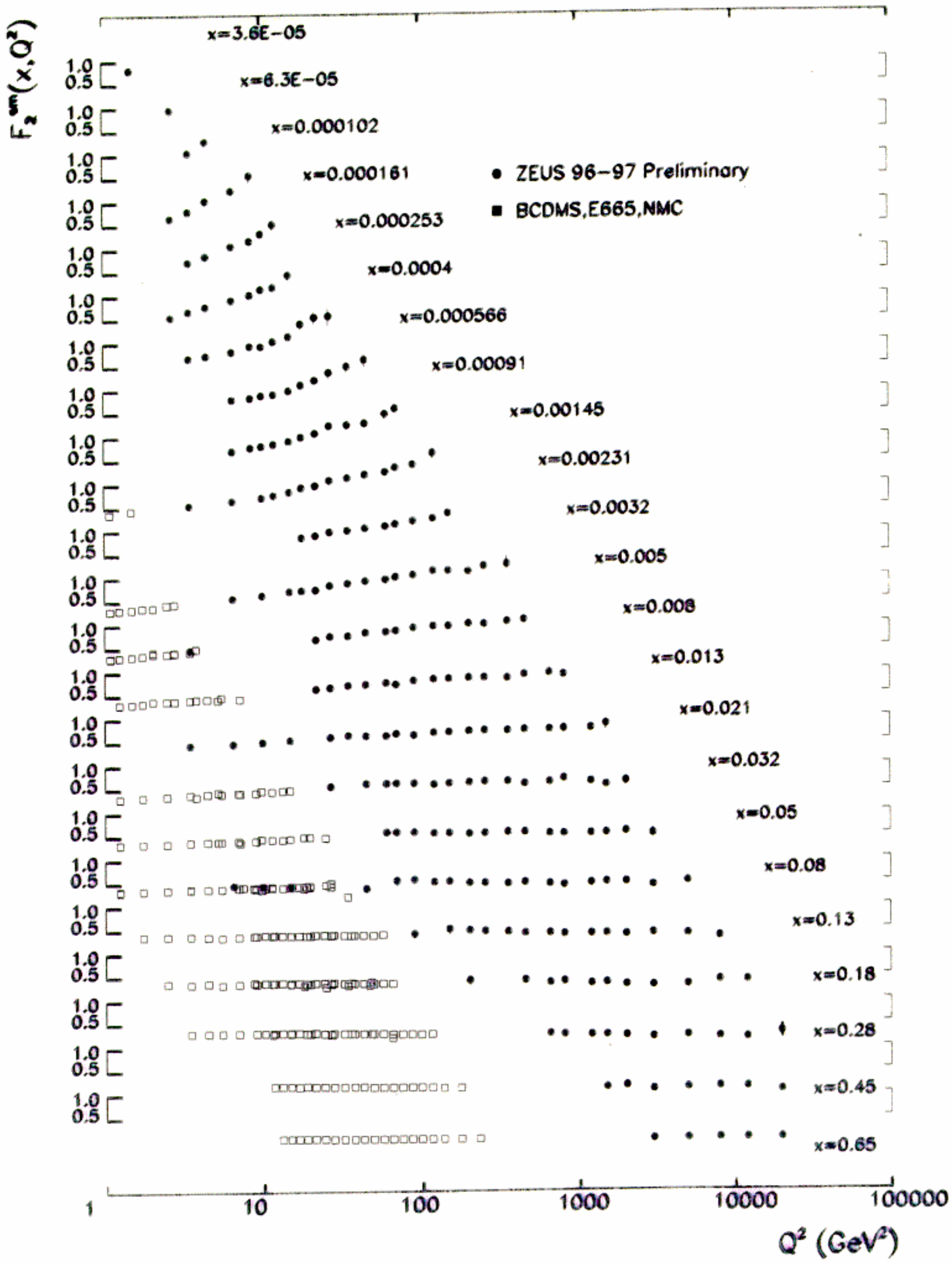

- Scaling is visible at $x \simeq 0.3$
- Scaling is violated at low x

$F_2(x, Q^2)$ vs Q^2 at low Q^2

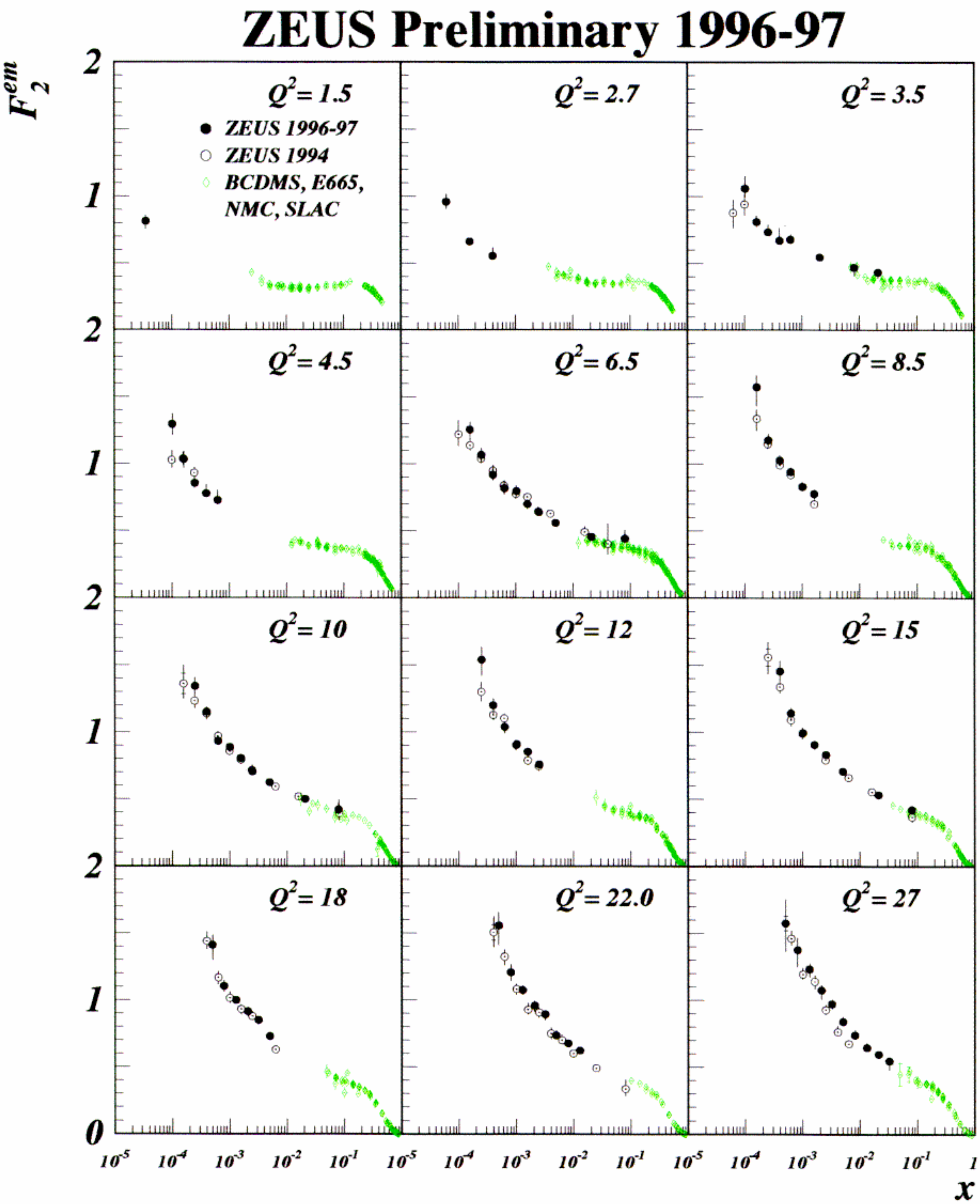

$F_2(x, Q^2)$ vs Q^2 at medium Q^2

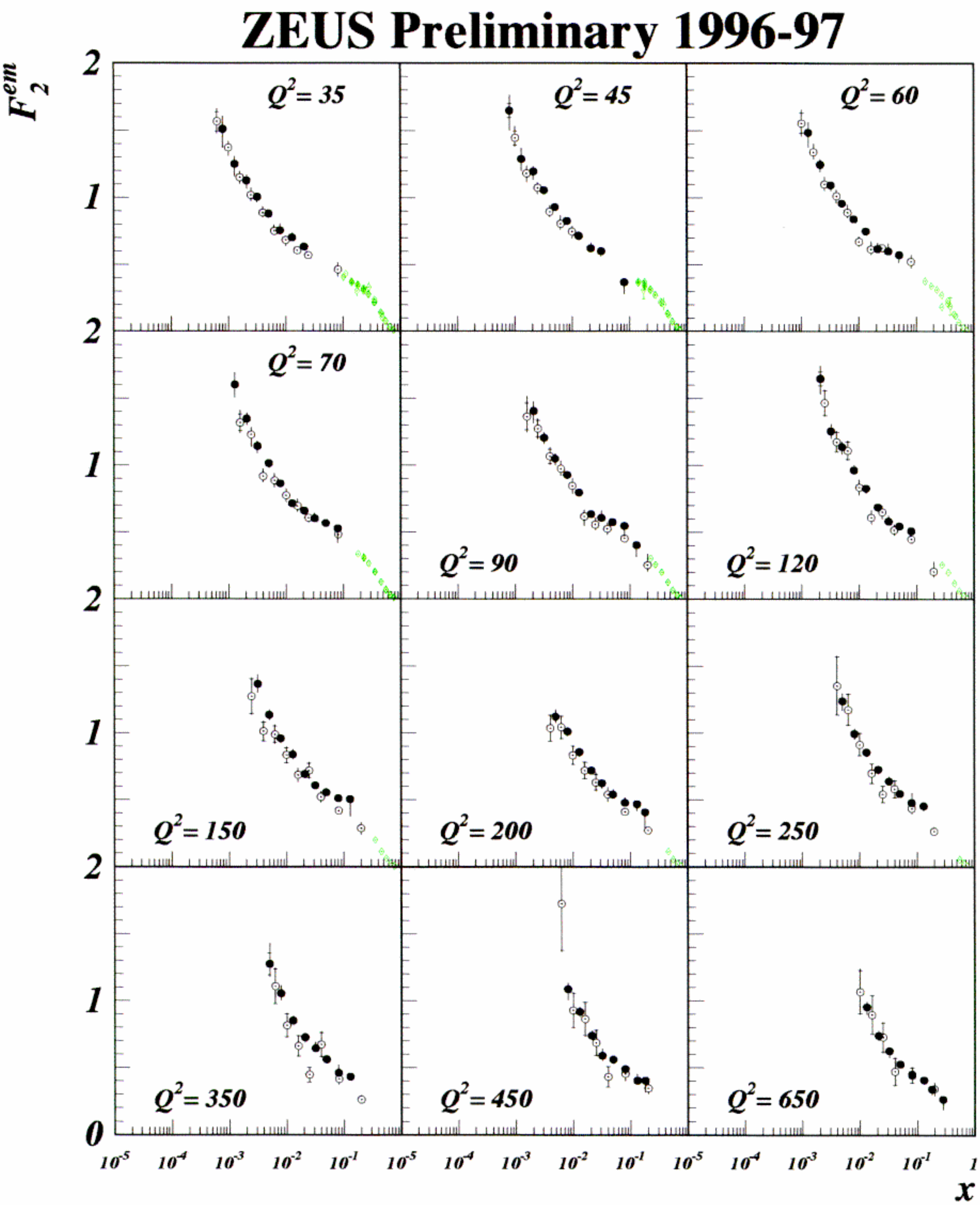

$F_2(x, Q^2)$ vs Q^2 at high Q^2

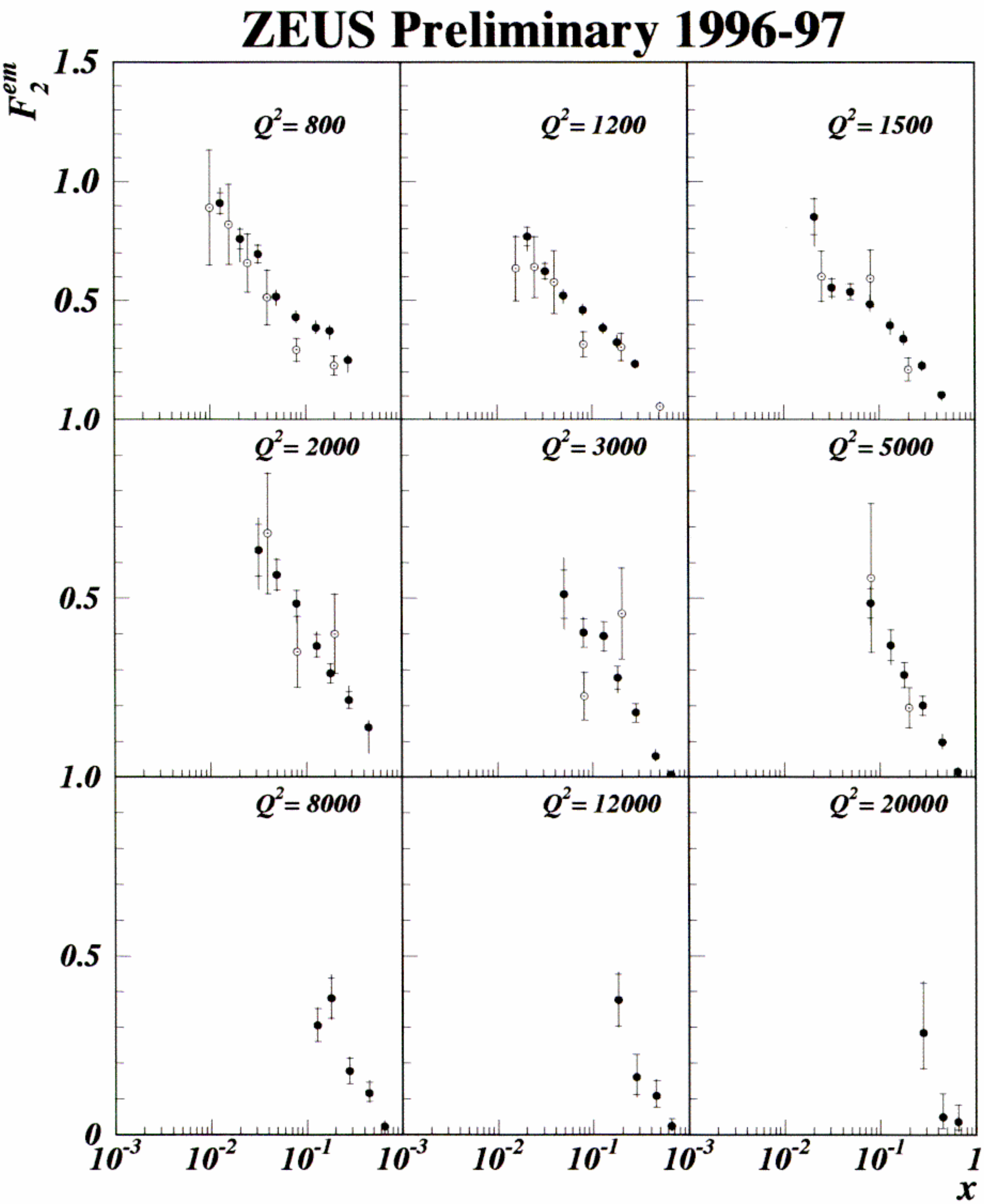

$F_2(x, Q^2)$ vs NLO QCD fit

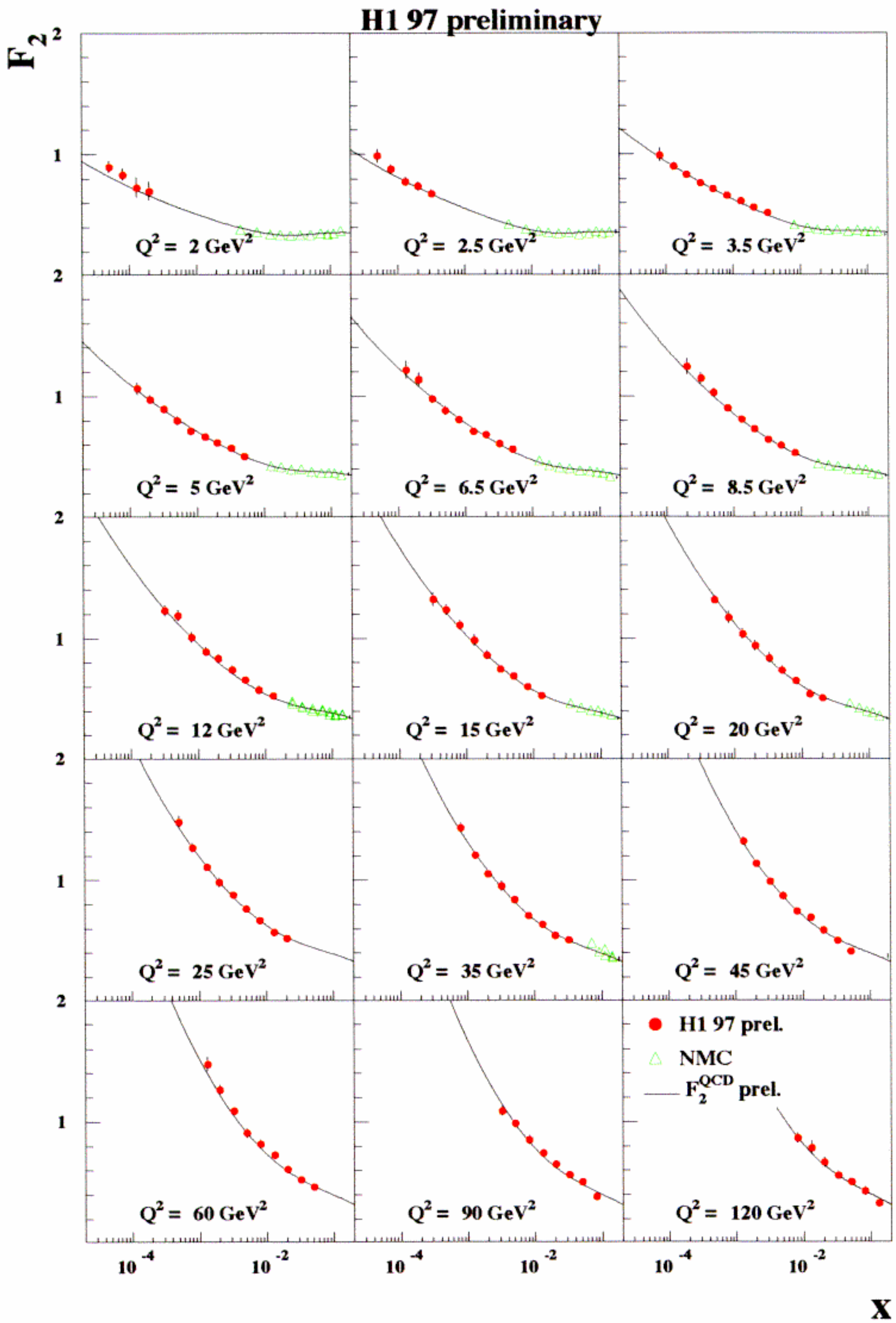

- F_L assumption based on QCD fit (small influence)
- Precision: $\simeq 1\%$ (stat) 3-4 % (syst)
- DGLAP describes the data very well...
  ...even at low Q^2 and low x!

Scaling Violations at Low x

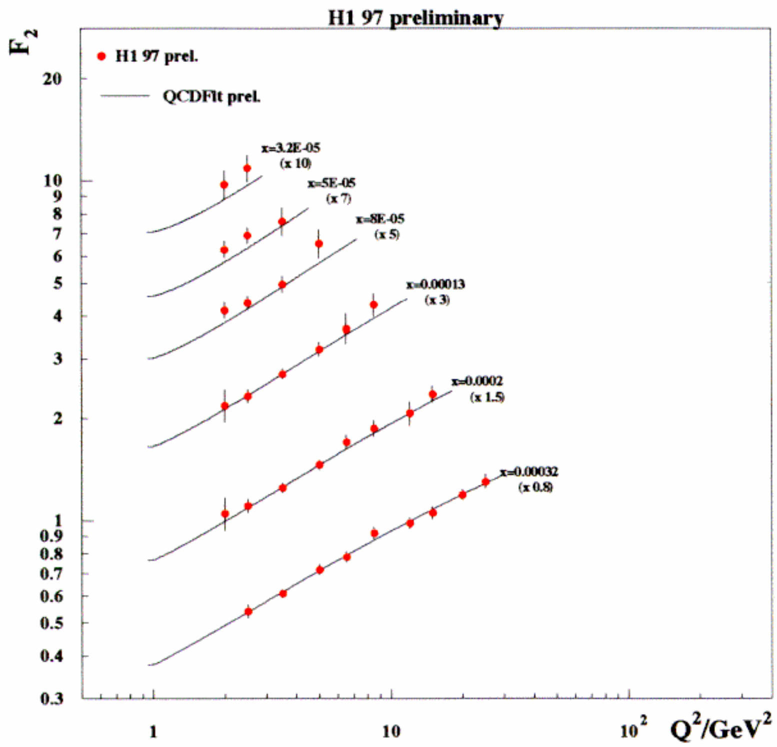

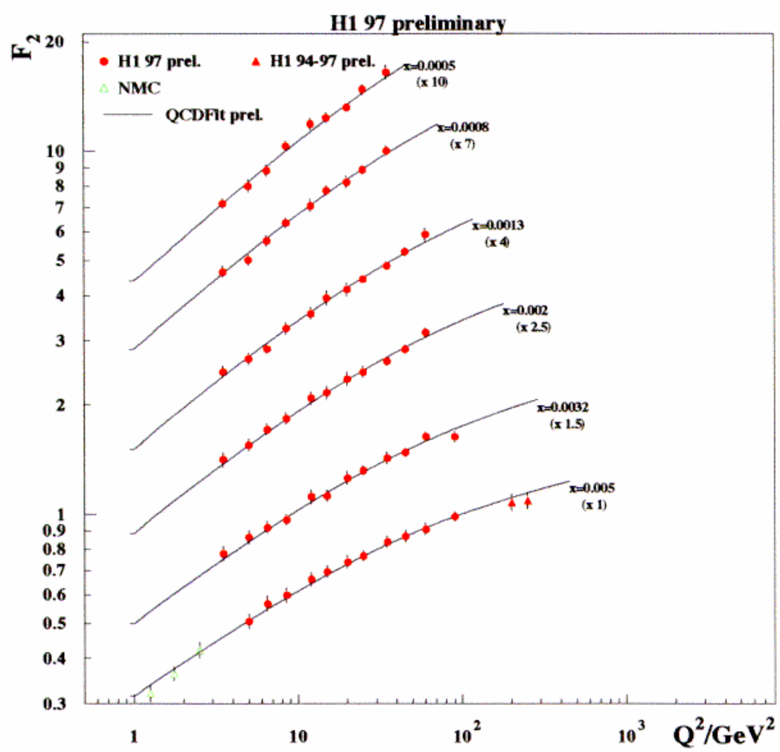

- Large slope $\mathrm{d}F_2/\mathrm{dln}\,Q^2$ at low x which stops increasing at $x \simeq 10^{-4}$
- Scaling violations due to large gluon radiation at low x

Towards Scaling at $x \simeq 0.1$

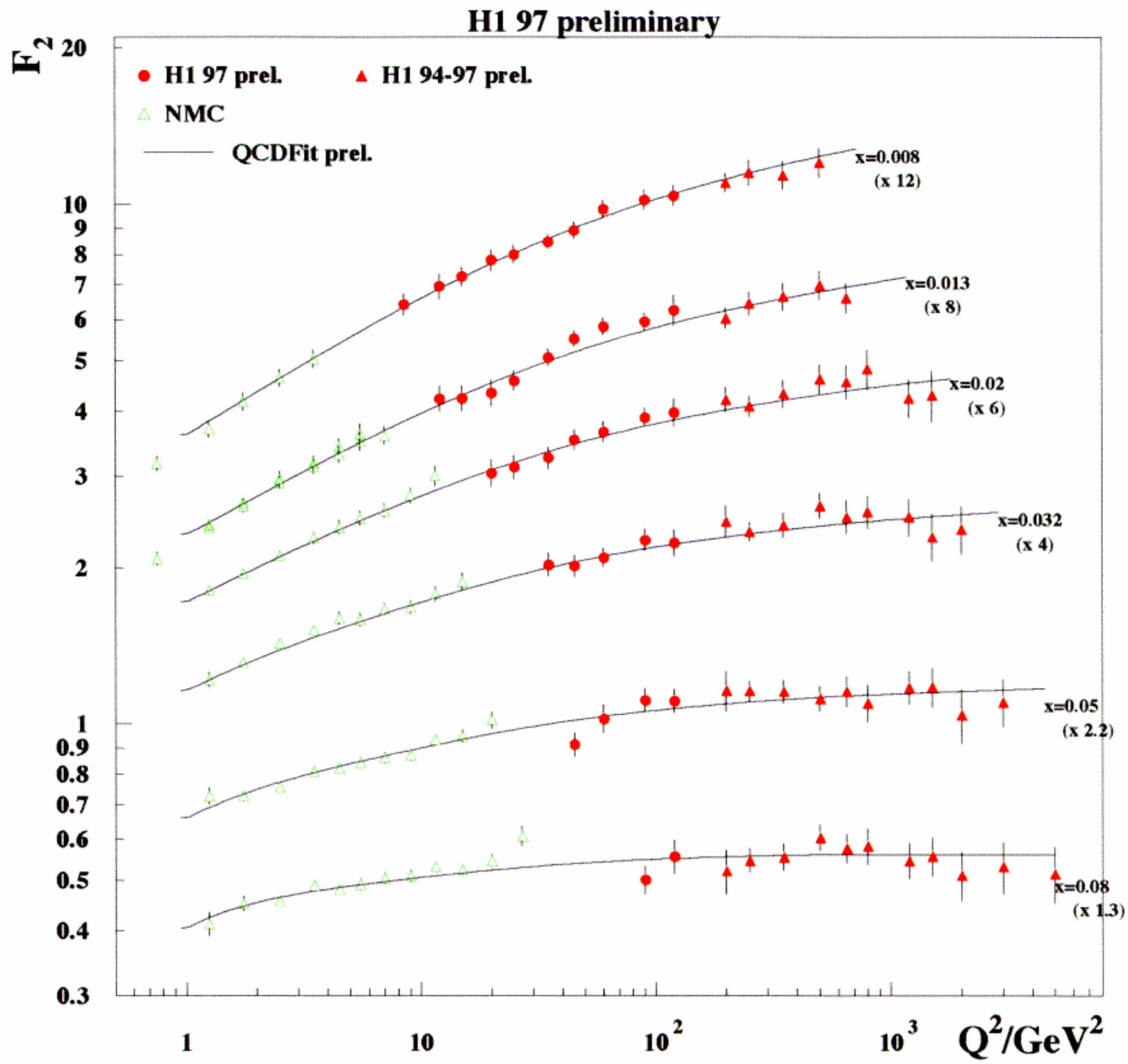

- Precision on F_2 at HERA now comparable to fixed target experiments (few %)
- Good agreement between the measurements of the fixed target experiments and HERA
- Scaling at $x \approx 0.1$ observed up to 5000 GeV^2

Scaling Violations at High x

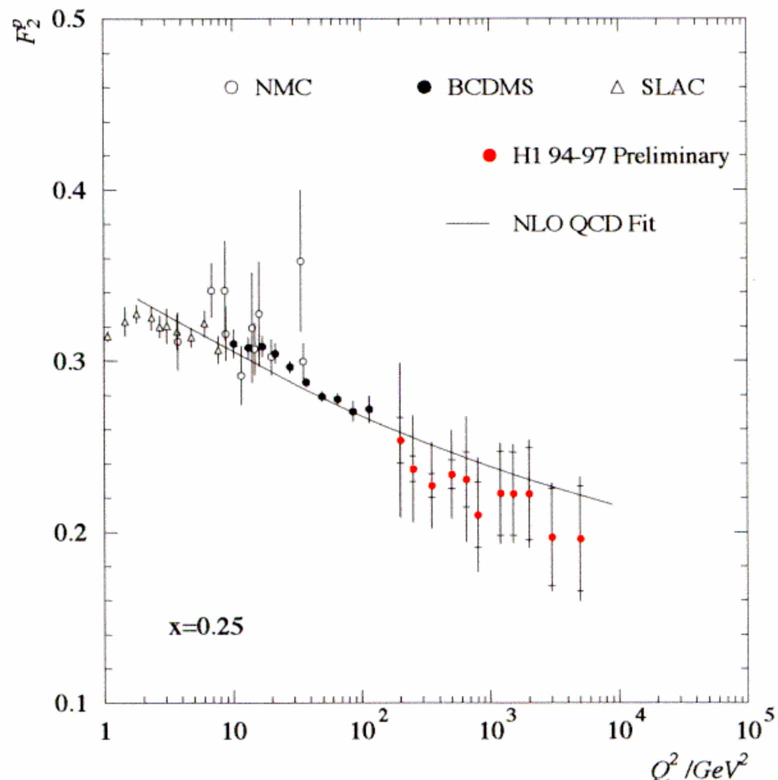

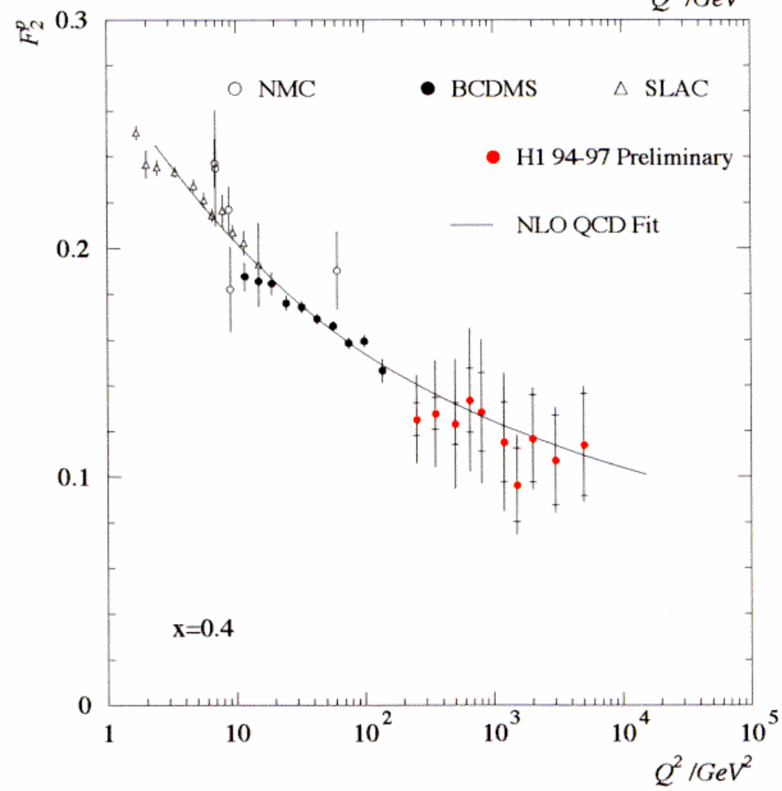

- Still large statistical error at high x, which is reachable at HERA only at $Q^2 \gtrsim 100$ GeV^2
- Good description of the data by NLO DGLAP fit.

Extraction of $\boldsymbol{F_L}$ from Cross-Sections

Reduced x-section: $$\frac{1}{\kappa}\frac{d^2\sigma}{dx dQ^2} = F_2 - \frac{y^2}{Y_+}F_L \equiv \sigma_{red} \equiv \tilde{\sigma}$$

with $\kappa = \frac{2\pi\alpha^2 Y_+}{Q^4 x}$ and $Y_+ = 1 + (1-y)^2$

$\Rightarrow$ subtract at high y: $$F_L = \frac{Y_+}{y^2}\left(F_2^{fit} - \frac{1}{\kappa}\frac{d^2\sigma^{exp}}{dx dQ^2}\right)$$

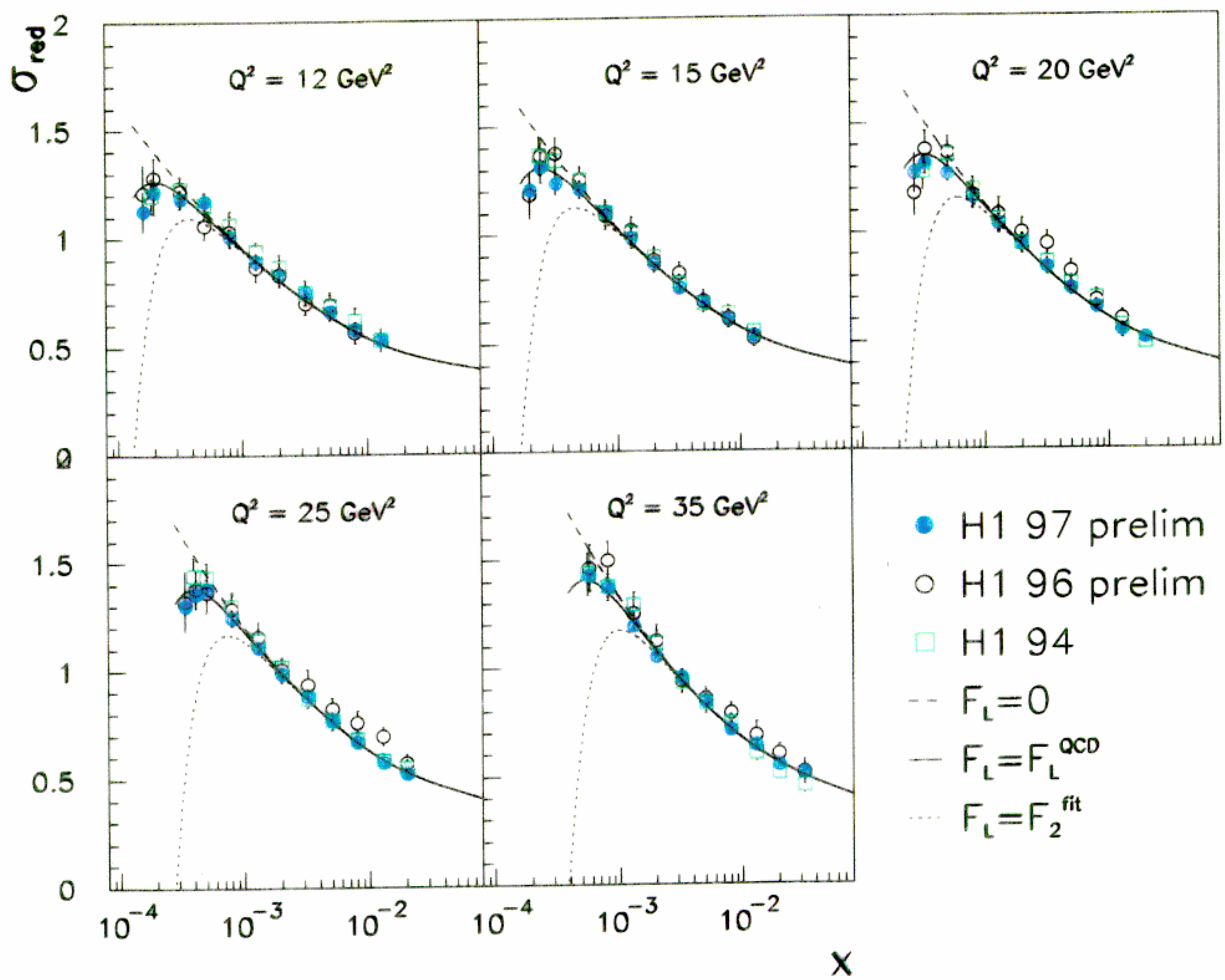

DGLAP NLO QCD fit to F_2 (H1-94..97, $y < 0.35$)

$\partial\tilde{\sigma}/\partial \ln y$: sensitive to F_L

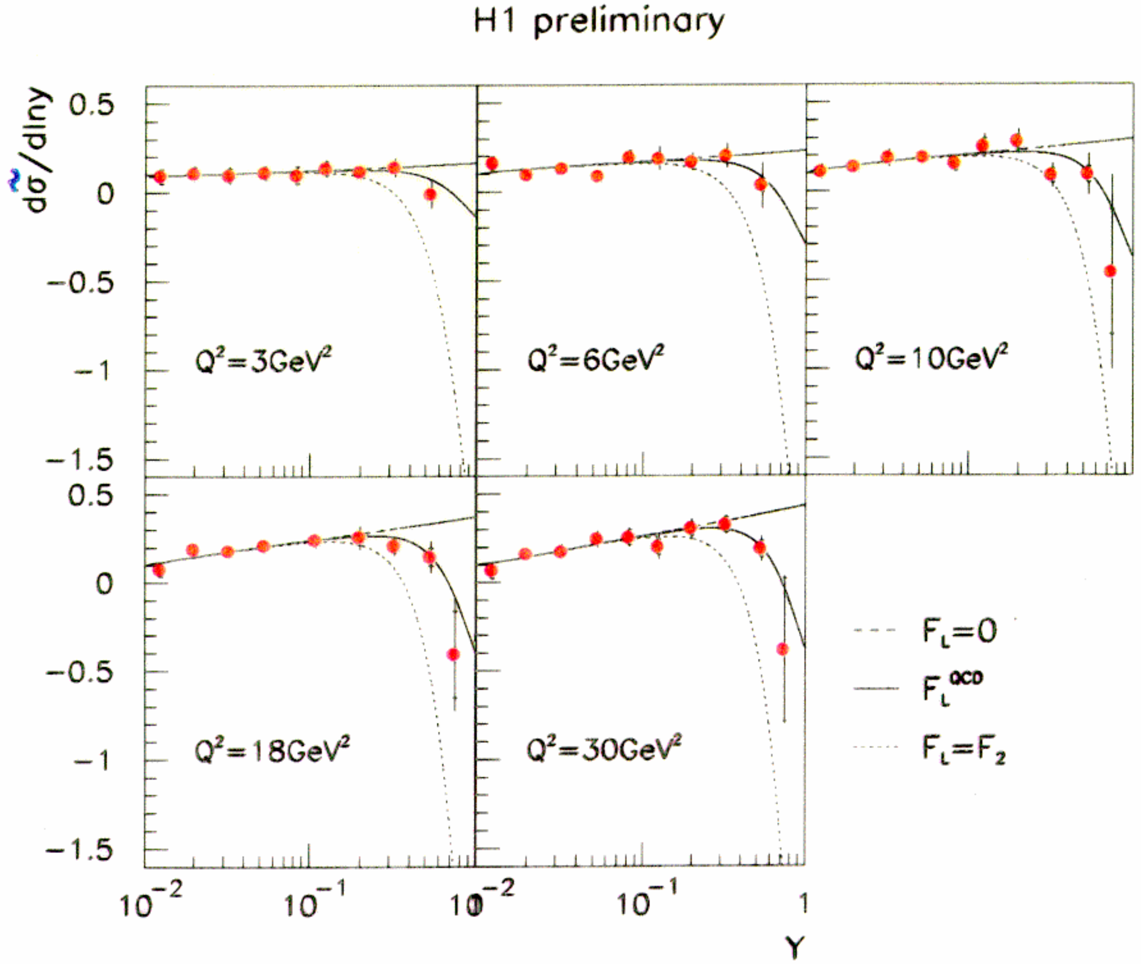

at fixed Q^2, we have:

$$\frac{\partial\tilde{\sigma}}{\partial \ln y} = -\frac{\partial F_2}{\partial \ln x} - F_L \cdot 2y^2 \cdot \frac{2-y}{Y_+^2} + \frac{\partial F_L}{\partial \ln x} \cdot \frac{y^2}{Y_+}$$

- assume $\partial F_2/\partial \ln y = A \ln y + B$
- Straight line fit to $\partial\tilde{\sigma}/\partial \ln y$ in Q^2 bins at $y < 0.2$

(This approximation has been checked with the QCD fit)

$\Rightarrow$ Access to lower Q^2 than with subtraction method
(No QCD extrapolation at low x, low Q^2)

Determination of the Longitudinal s.f. F_L

Two methods used for the F_L determination:
The subtraction method (•) and the derivative method(⋆)

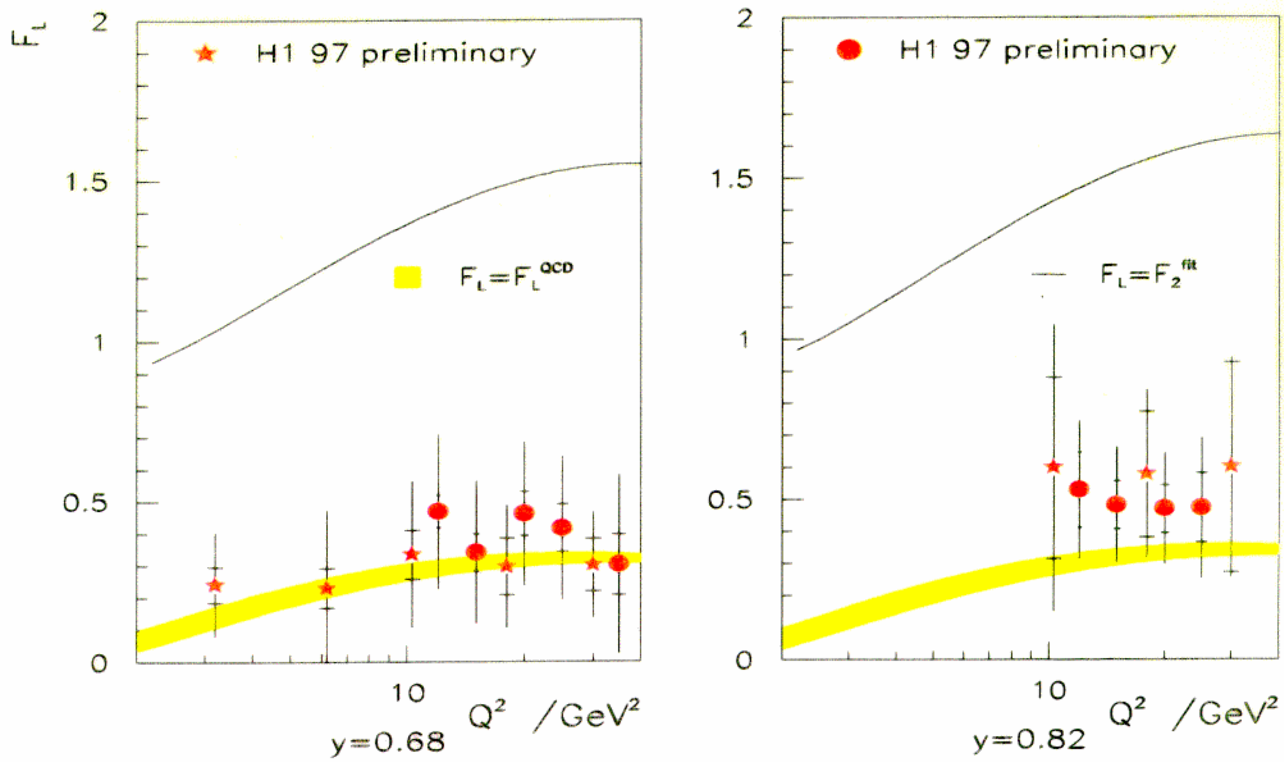

- Extracted F_L compatible with QCD prediction
- Good agreement between the two extraction methods, which use the same data but different characteristics of the F_2 and F_L behaviour.
- Slight tendency of $F_L^{H1} > F_L^{QCD}$ at the highest y

Note: the systematic errors of the points at the same y are correlated

Future: Measure F_L Directly by Changing Beam Energies

The Charm Contribution to F_2

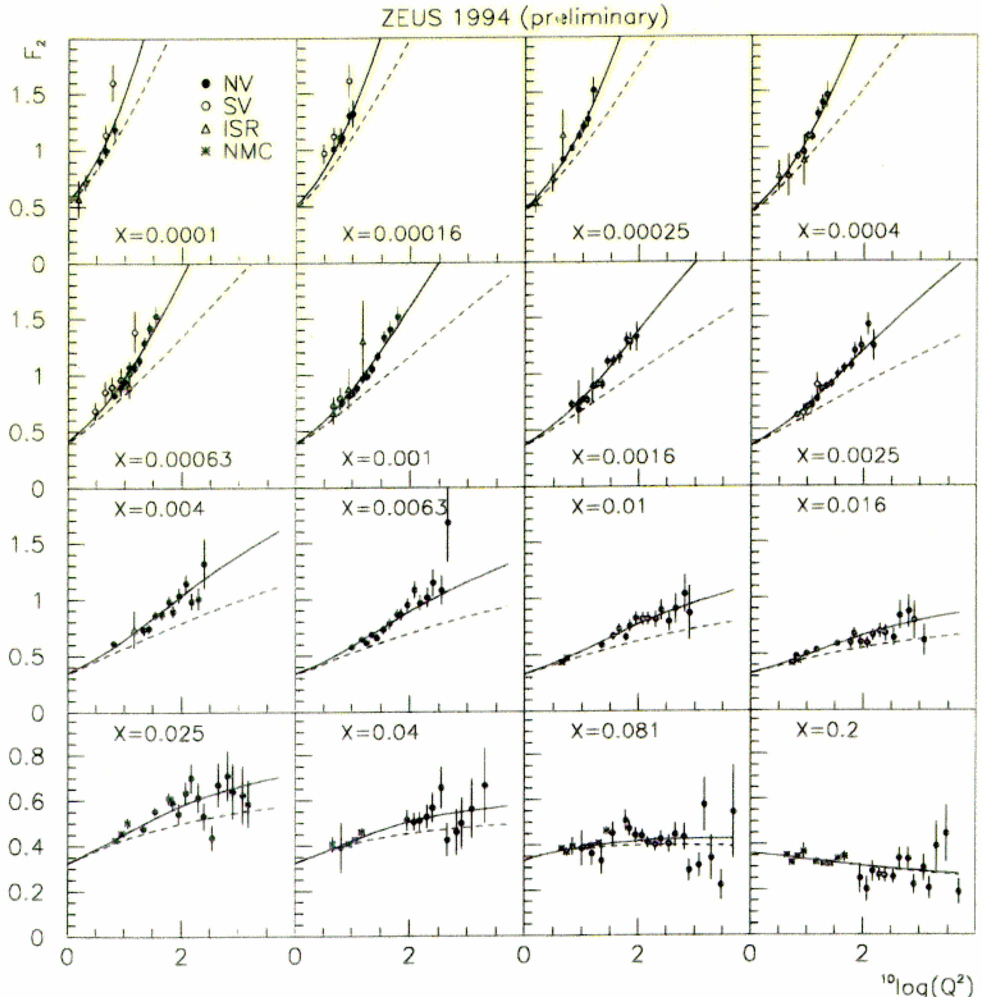

— $F_2 = F_2^{u,d,s} + F_2^c$ - - - $F_2 = F_2^{u,d,s}$

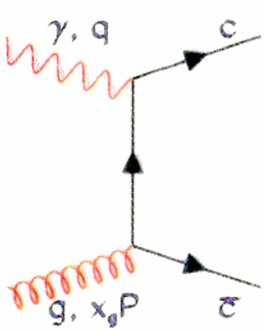

- F_2^c from Boson-Gluon-Fusion generated dynamically m_c taken into account
- charm contribution up to ~ 25 %

Can we measure it directly?

Charm in DIS

Select in DIS sample ($1 < Q^2 < 600$ GeV^2, $0.02 < y < 0.7$)

$D^{*+} \to D^0\pi^+ \to (K^-\pi^+)\pi^+ + c.c., with$

$M(K\pi) : 1.80 - 1.92$ GeV ; $M(K\pi\pi) - M(K\pi) : 143 - 148$ M

$1.5 < p_T(D^*) < 15$ GeV,

$\Rightarrow \sigma(ep \to eD^*X) = 8.55 \pm 0.40^{+0.30}_{-0.24}$ nb

ZEUS PRELIMINARY 96-97

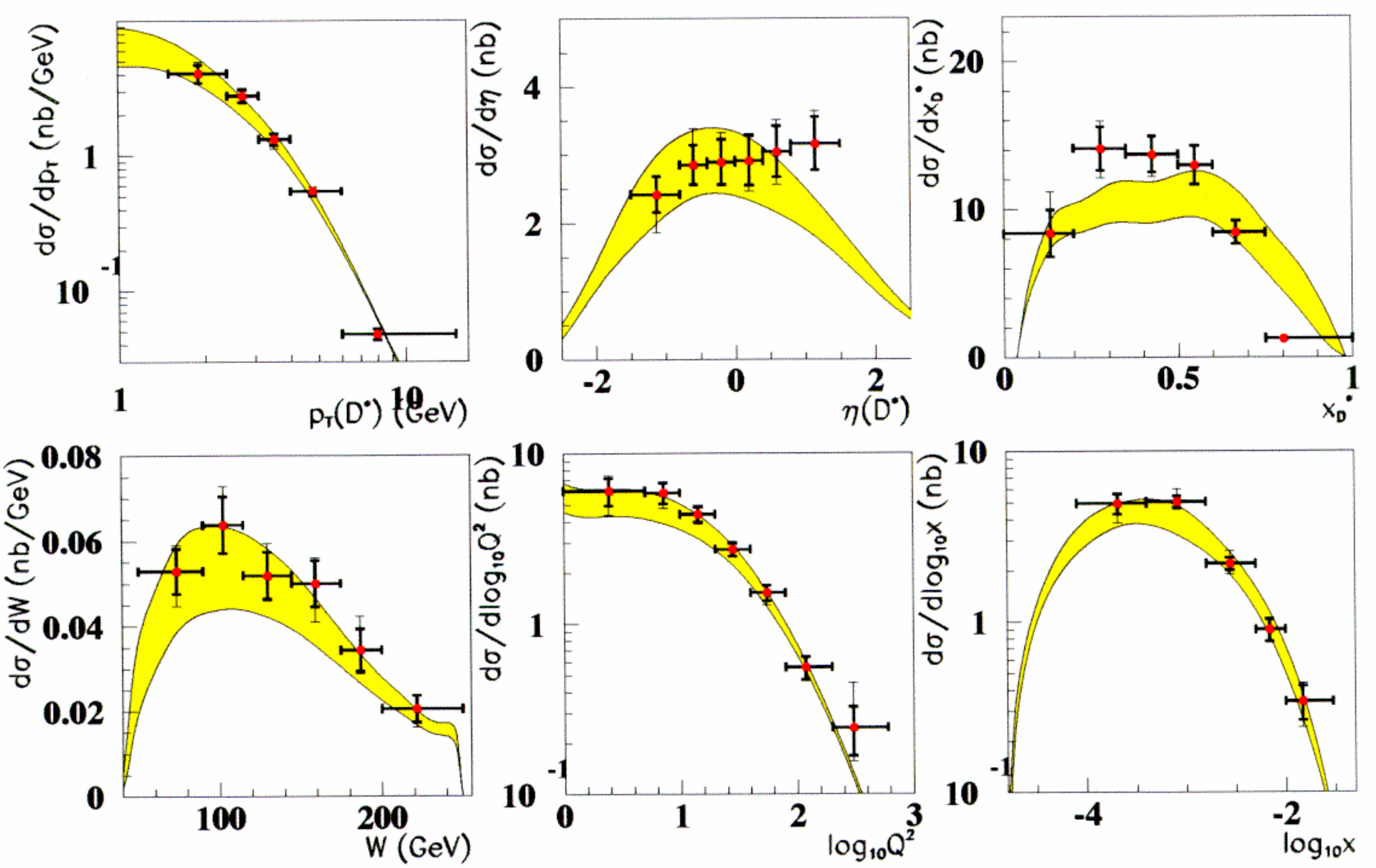

$\Rightarrow$ agreement with "massive" NLO pQCD calculation except

high-η ? **low-$x(D^*)$?**

Measurement of $F_2^{c\bar{c}}$:

$$\frac{d^2\sigma_{c\bar{c}X}}{dx\,dQ^2} = \frac{2\pi\alpha^2}{xQ^4}\left[1 + (1-y)^2\right]F_2^{c\bar{c}}(x, Q^2)$$

Extraction of $F_2^{c\bar{c}}$ requires: extrapolation to full $\{\eta, p_T\}$ range.

– fragmentation functions $c \to D$

– $F_L^{c\bar{c}}$ is small and neglected

ZEUS PRELIMINARY 95-97

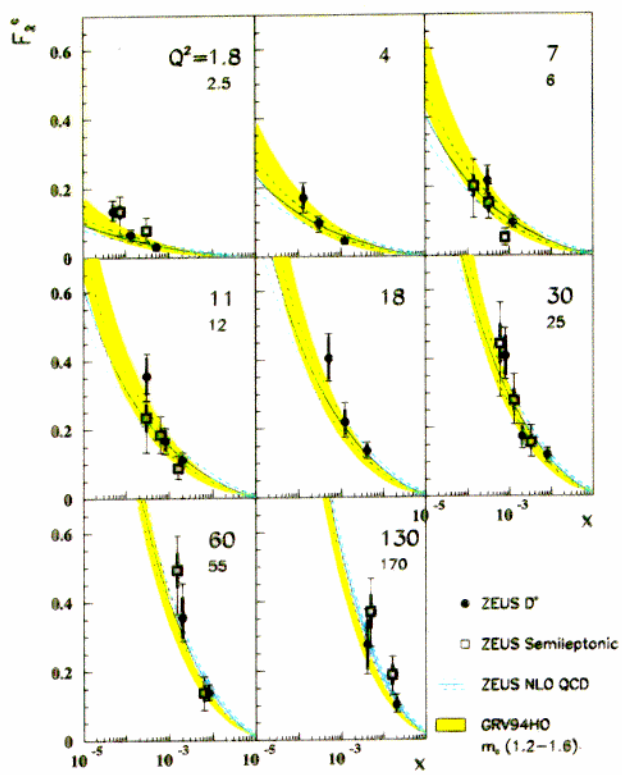

- Precision $\simeq 15 - 20\%$
- Significantly more precise than earlier measurements
- Steep rise towards small $x \to$ gluons
- Good agreement between direct measurement and indirect prediction from perturbative QCD

The Gluon Density from the Charm

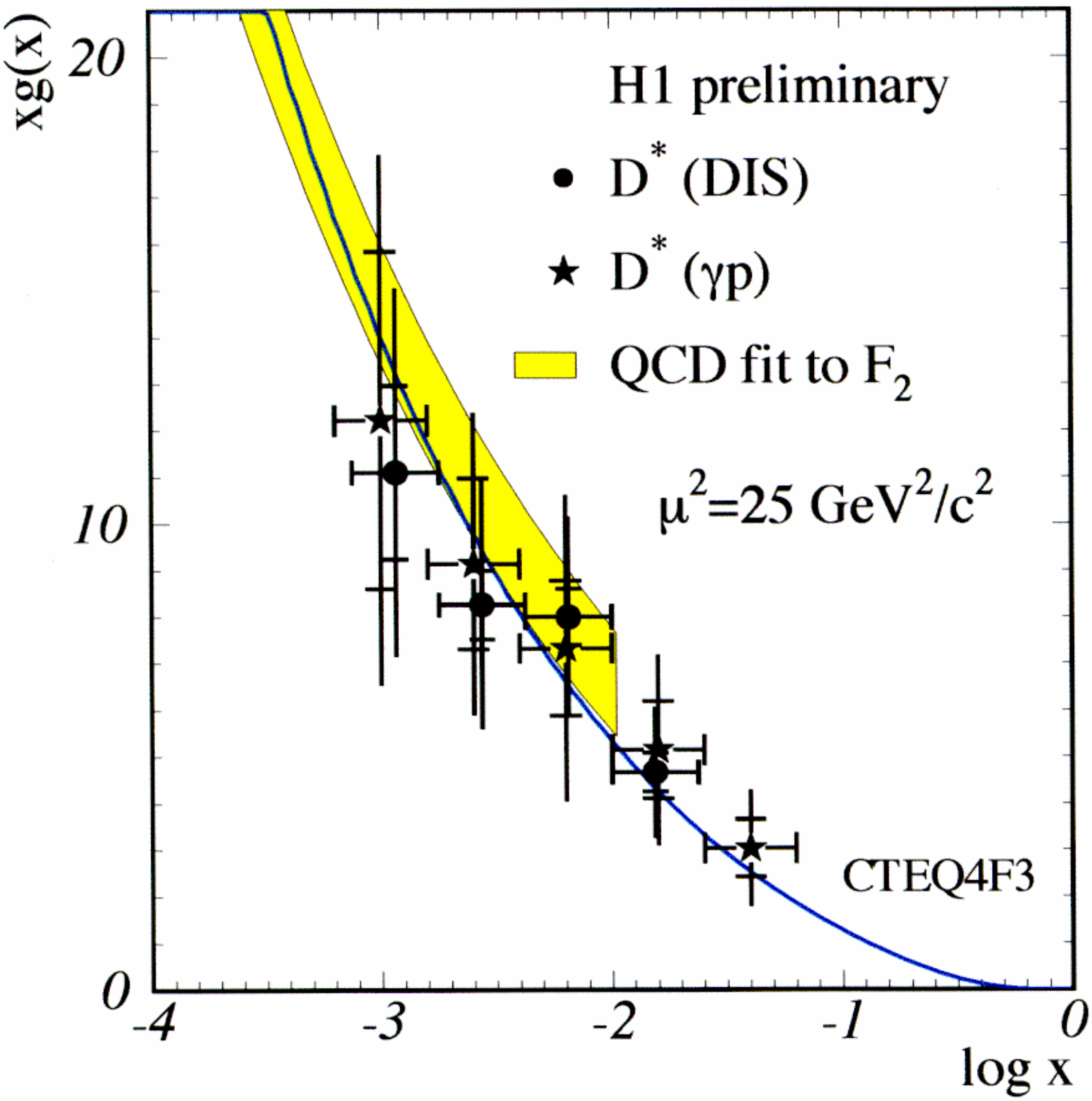

- The extraction of the gluon density from the direct measurement of the D^* production cross-section in DIS is in agreement with the gluon density obtained from the QCD fit to the inclusive cross-sections.
- Similar result from the direct measurement of the D^* production cross-section in photoproduction.

The Gluon Density from NLO QCD fit

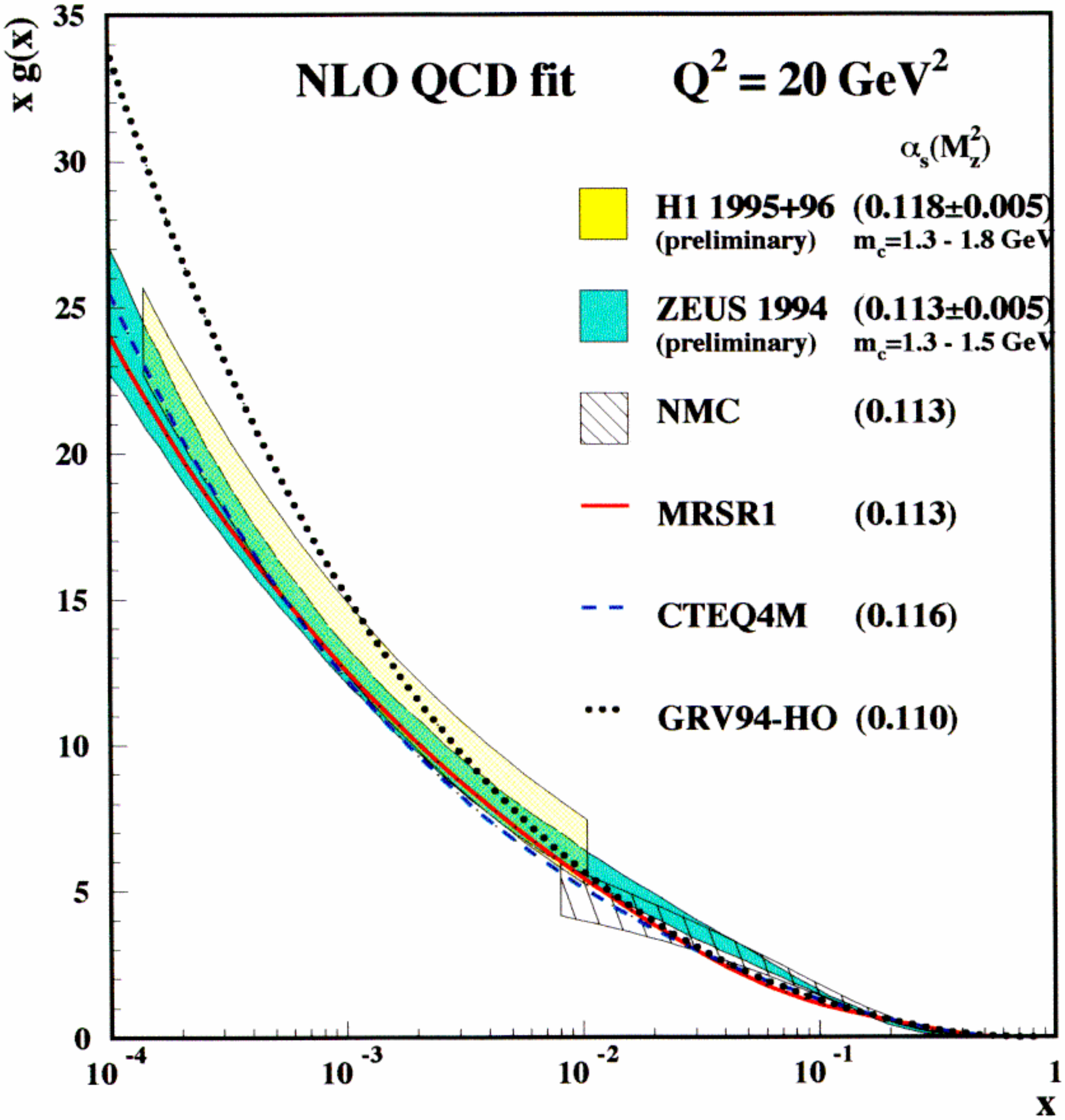

- steep rise of xg for decreasing x
- good agreement between H1 and ZEUS
- error band takes correlated systematics into account
- precision at $x \sim 5 \cdot 10^{-4}$: $\sim 15\%$
- H1 and ZEUS are consistent with MRSR1 and CTEQ4M
- GRV too steep, but uses a lower α_S value

Gluon and Sea-Quarks Densities

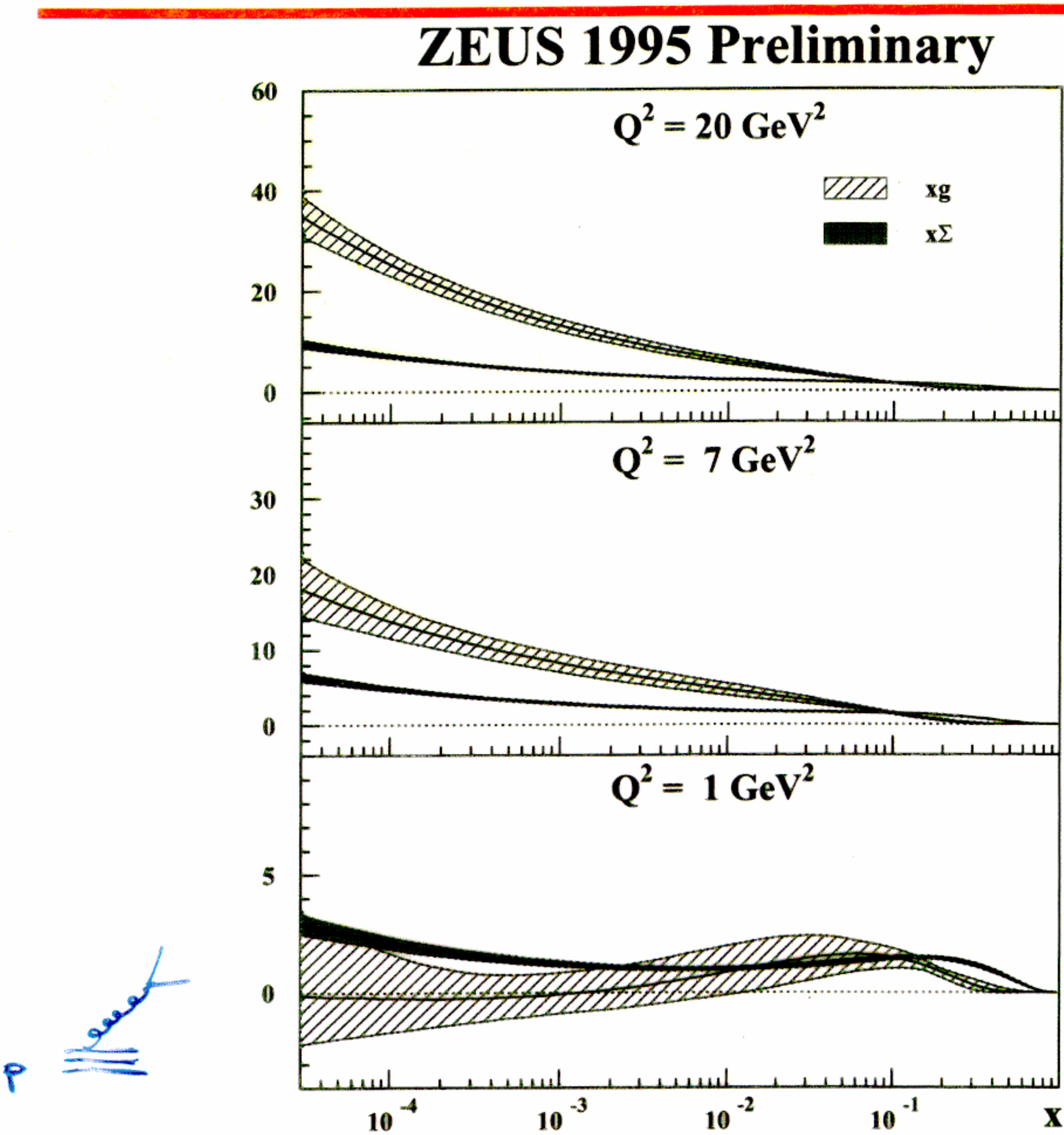

- xg is steeper at low x than the Sea-quarks density at Q^2 greater than a few GeV^2
- xg is almost flat at 1 GeV^2, while the Sea-quarks density is already increasing at low x
- Difference of dynamics at $Q^2 \lesssim 1\ GeV^2$?

The Gluon from the Dijet Cross-Section

fit: $\frac{d^2\sigma_{dijet}}{dQ^2 d\xi}$ with $\xi = x\left(1 + \frac{M_{jj}^2}{Q^2}\right)$

and $\frac{d^2\sigma}{dx dQ^2}$

data $200 \leq Q^2 \leq 5000$ GeV^2

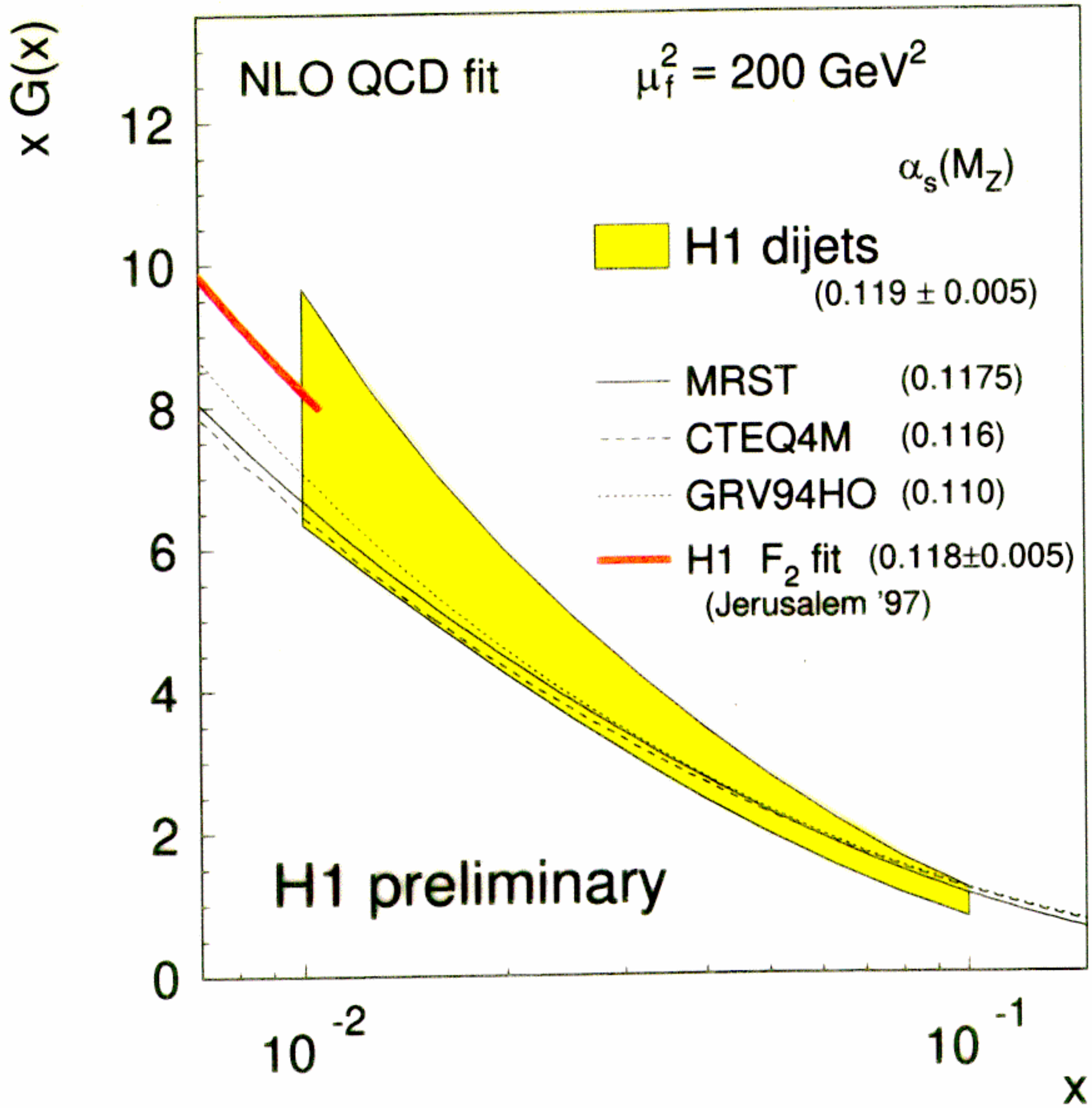

Gluon density obtained is consistent with xg determined

Jets at HERA

- Jets

→ Gluon density from jets

→ Jet shapes in DIS

→ Measurement of α_S:

from integrated jet rates

from differential jet rates

from event shapes

Processes in $O(\alpha_s)$

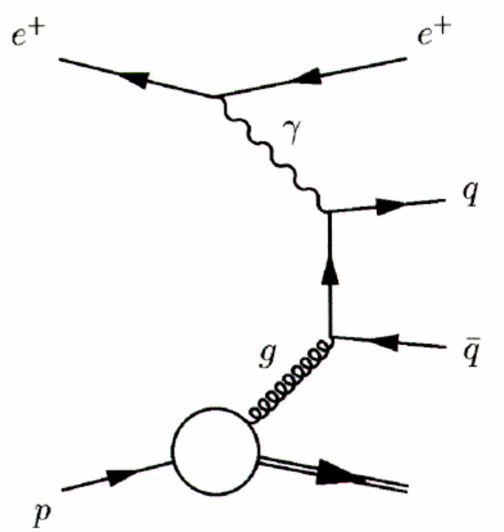

Boson–Gluon–Fusion

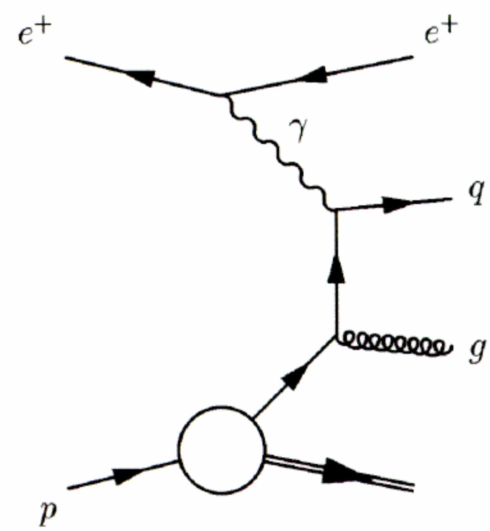

QCD–Compton

Jet shape variable

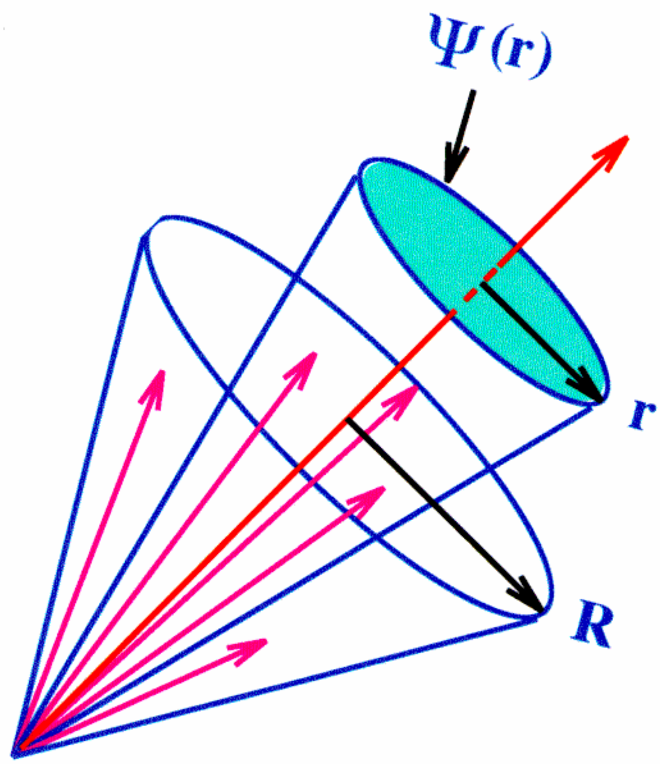

- $\Psi(r)$: average fraction of transverse jet energy contained in a cone of radius r
- by construction: $\Psi(r = R) = 1, \quad \Psi(r = 0) = 0$

Jet selection

- (CDF) cone algorithm, cone radius $R = 1$
- the jets are constructed from calorimeter energy depositions
- $-1 < \eta^{jet} < 2$

Comparison with e^+e^- and $p\bar{p}$

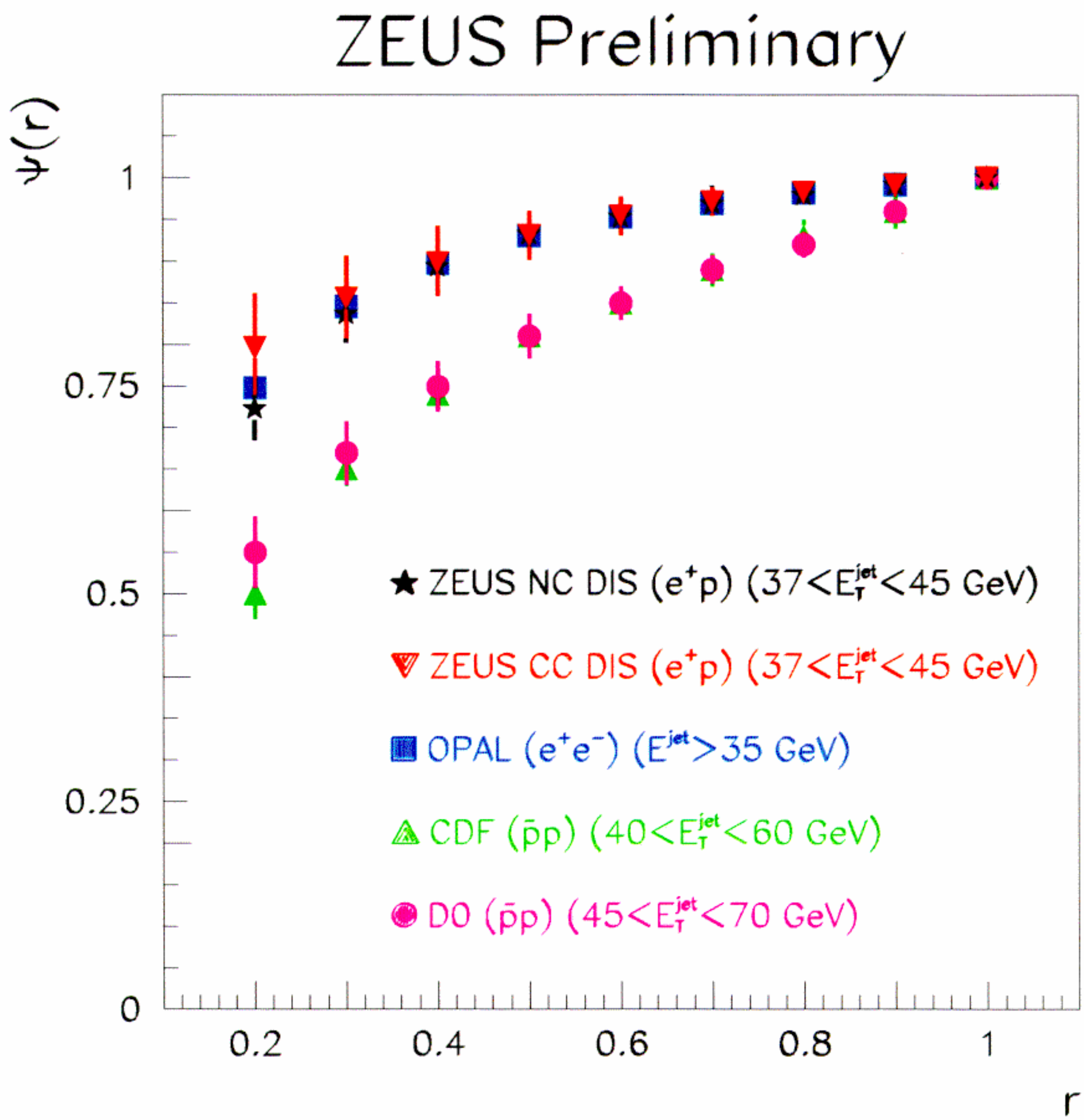

- selection of jets with comparable (transverse) energies
  ZEUS (DIS) and OPAL: mostly quark jets
  CDF and D0: mostly gluon jets
- jet profiles from ZEUS are very similar to OPAL
- jet shapes from ZEUS/OPAL are significantly narrower than those from CDF/D0

Comparison of DIS and Photoproduction

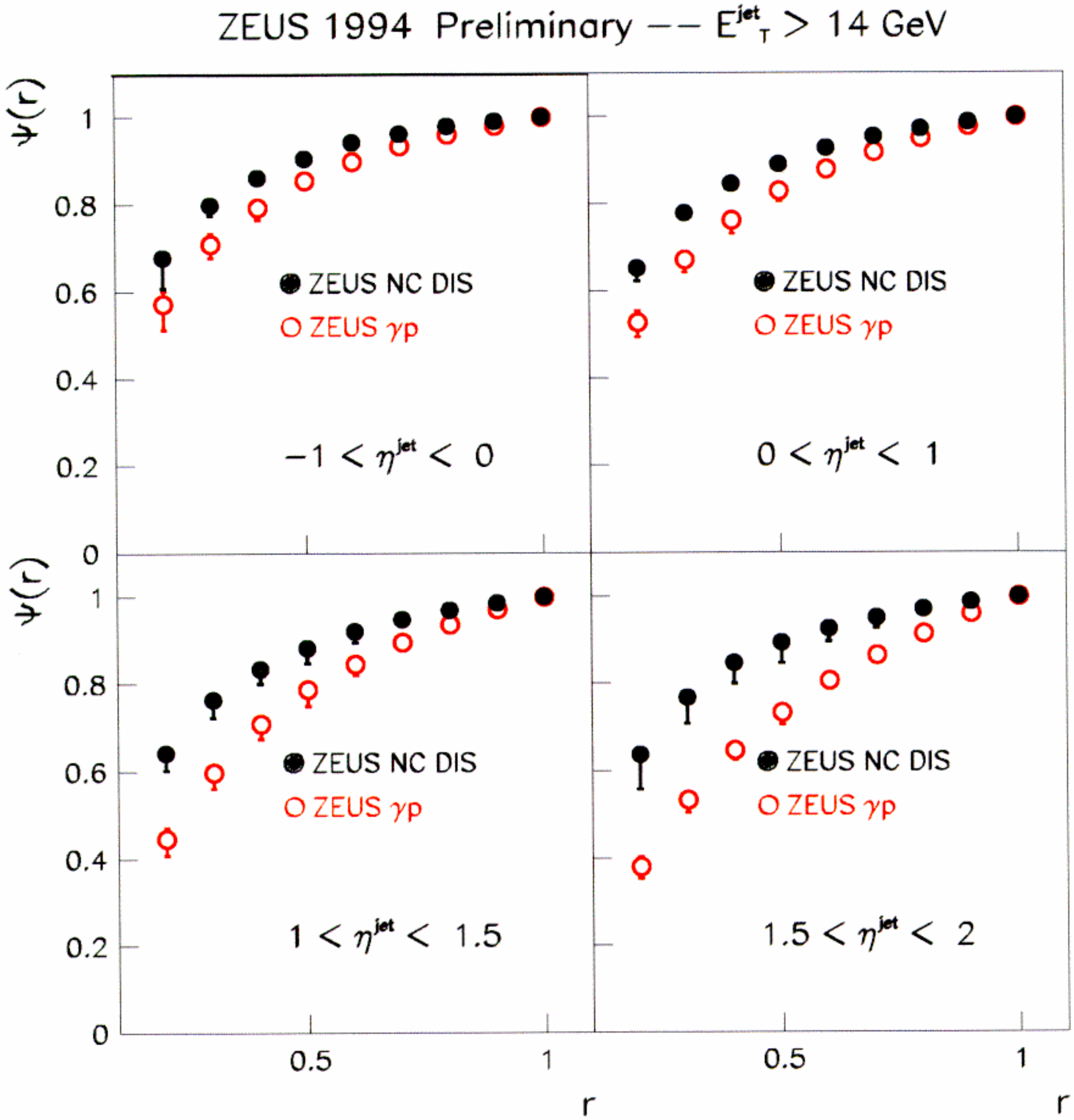

average over jets with $E_t > 14$ GeV

- clear difference between jets from DIS and photoproduction
- diffference increases with η^{jet}
- interpretation: gluon jets from resolved photoproduction dominant at large η^{jet}

(JADE) Jet Algorithm

- remove scattered electron;
  add missing momentum 'pseudo particle'

  successive combination of pairs of particles/clusters

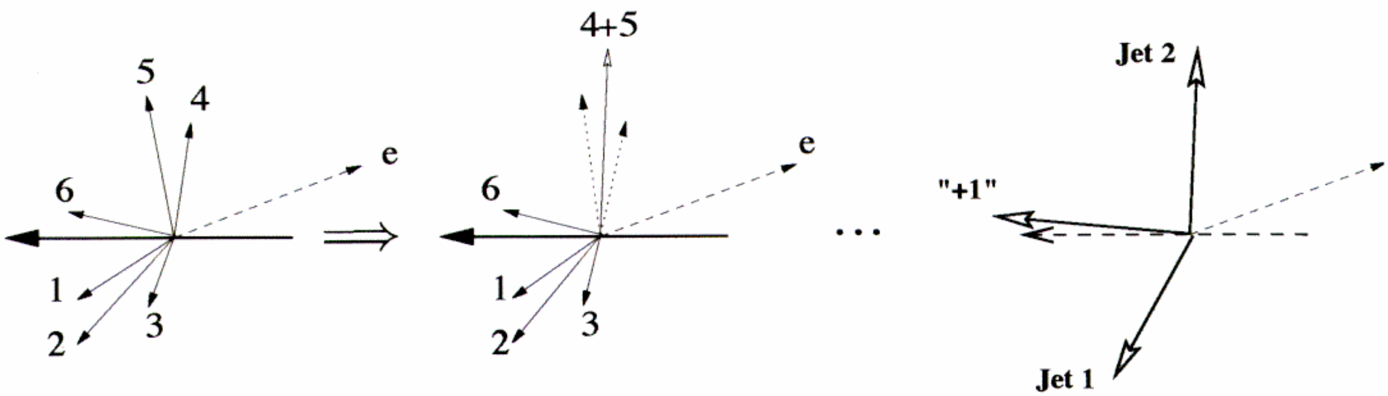

- which particles are combined ?

  'distance/resolution criterion' d_{ij}^2 JADE: $d_{ij}^2 = 2E_iE_j(1 - \cos\theta_{ij})$

- in which way are the particles combined ?

  'recombination scheme' JADE: $p_{comb} = p_i + p_i$

- when does the iteration stop ?

  'integrated' jet rate: no pair of particles/jets is left
  with $d_{ij}^2/W^2 \; < \; y_{cut}$; $R_{2+1}(Q^2) \equiv N_{2+1}(Q^2)/N_{DIS}(Q^2)$

  'differential' jet rate: (2+1) jets are left; $y_2 \equiv \min d_{ij}^2/W^2$

'Integrated' (2+1) jet rate $\boldsymbol{R_{2+1}(Q^2)}$

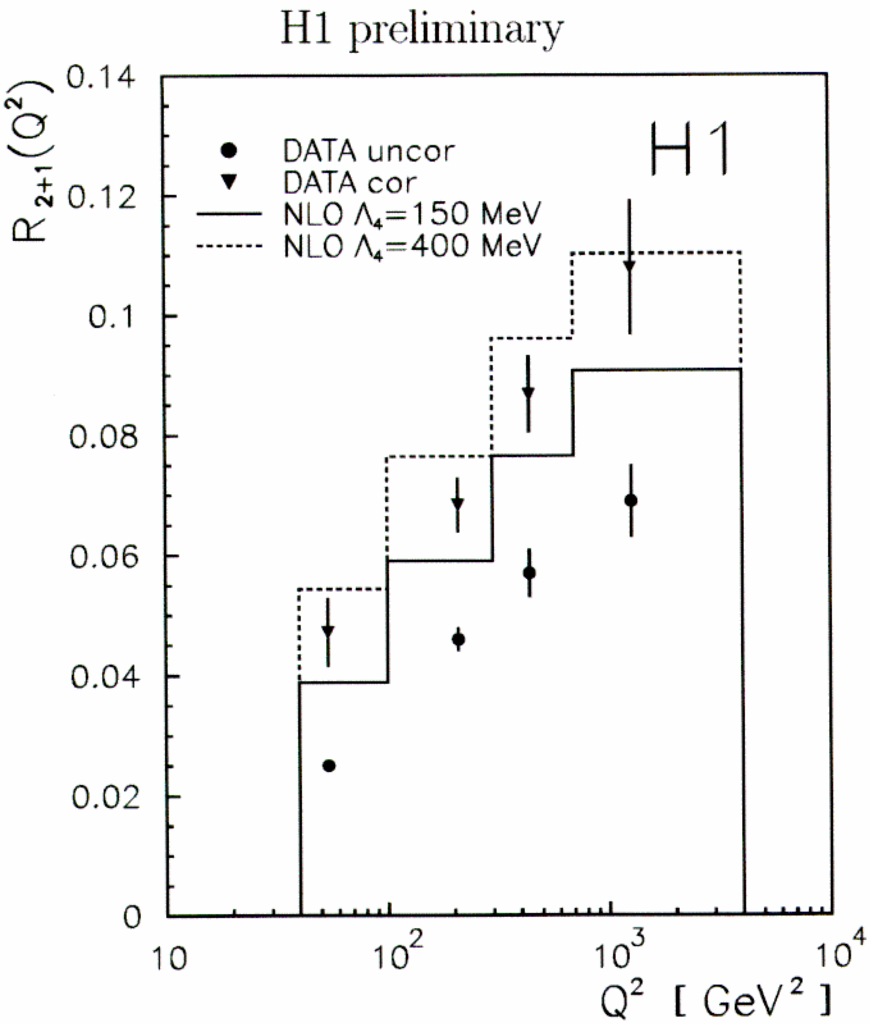

- the 3-jet rate $R_3(s)$ in e^+e^- annihilation is **the method** to measure ~~the running of~~ α_S!

- **aim at HERA:** demonstration of the running of α_S with one method in one experiment to minimize the systematic uncertainties by measuring $R_{2+1}(Q^2)$

- Correction factors for detector and hadronization effects are (still) large: $\sim 1.5 - 1.9$ in particular at low Q^2

- $R_{2+1}(Q^2)$ rises with increasing Q^2:

  $$R_{2+1}(Q^2) = A(Q^2, y_{cut})\alpha_s(Q^2) + B(Q^2, y_{cut})\alpha_S^2(Q^2))$$

  in $e^+e^- \to q\bar{q}g$: $R_3(y_{cut}) = A(y_{cut})\alpha_S(s) + B(y_{cut})\alpha_S^2(s)$

- Choice of renormalisation scale μ_R^2 in bin i is $\langle Q^2 \rangle_i$

'Running' of $\alpha_S(Q^2)$ from $R_{2+1}(Q^2)$

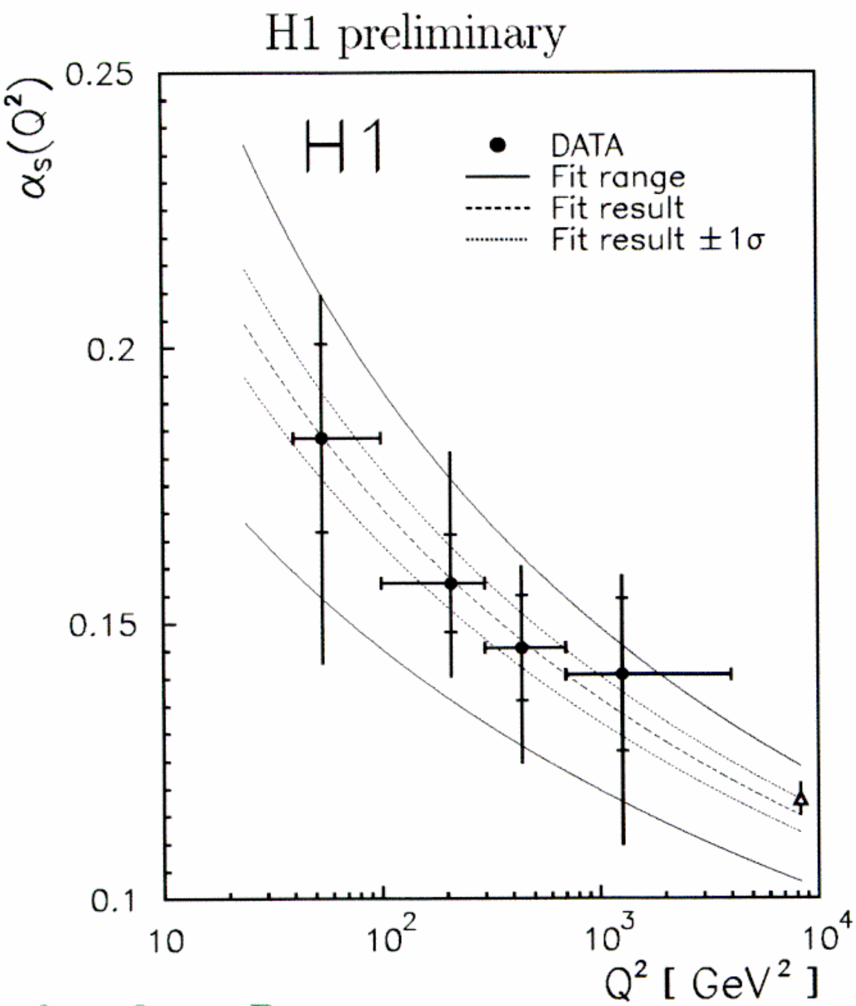

- result of α_s fit to R_{2+1}:
  4 values of $\alpha_s(< Q^2 >)$ corresponding to 4 bins of Q^2
- systematic uncertainties are largest at low Q^2
- (still) large statistical error at very high Q^2
  ($\Delta\alpha_s \sim 10\%$ for $700 < Q^2 < 4\,000$ GeV^2)
- unambiguous demonstration of 'running' of α_s is not (yet) possible
- averaging over full range of Q^2, we get:
  $\alpha_s(M_Z) = 0.115 \pm 0.003\ (stat.)\ ^{+0.008}_{-0.011}\ (syst.)$

'Differential' (2+1) Jet Rate

- differential 3–jet rates have been studied in much detail in e^+e^-–annihilation

- this is the first study of the corresponding variable in ep

  e^+e^-: *fixed* $s \Leftrightarrow$ ep: *range* of Q^2

- y_2 is complementary to $R_{2+1}\,(Q^2)$ at *fixed* jet resolution parameter y_{cut}

  within a given Q^2 range: $-\dfrac{dR_{2+1}}{dy_{cut}} = -\dfrac{1}{N_{tot}} \cdot \dfrac{dN_{2+1}}{dy_{cut}} \approx \dfrac{1}{N_{tot}} \cdot \dfrac{dN}{dy_2}$

- only the combined study of y_2 and $R_{2+1}\,(Q^2)$ gives the full picture of (2+1) jet rates at HERA

- analysis is restricted to $Q^2 > 200$ GeV^2

  $\Rightarrow$ reduced systematic uncertainties due to:
  suppression of initial–state QCD radiation;
  improved containment of jets in detector;
  better knowledge of parton densities at high x;
  …

α_s from Differential Jet Rate

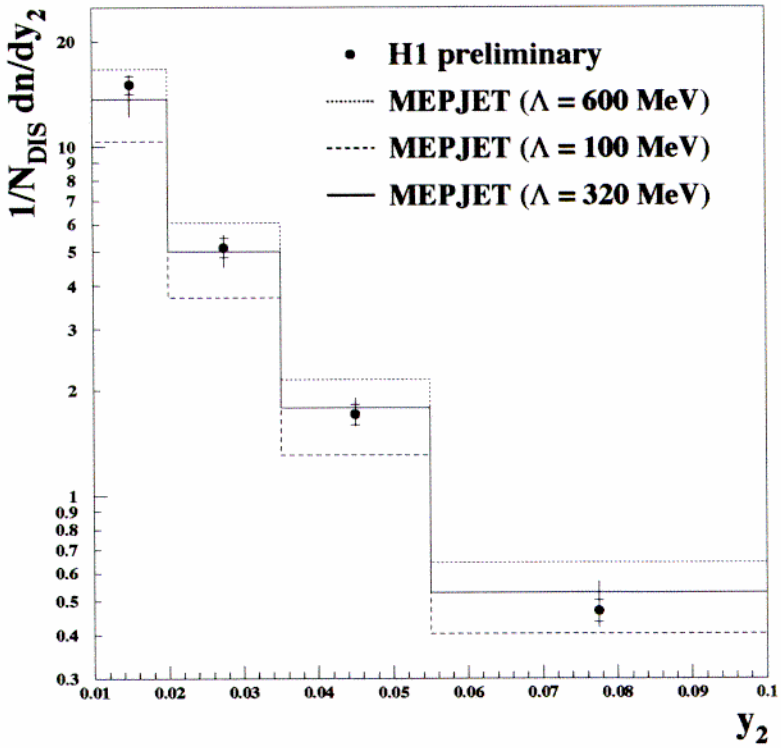

- $\Lambda_{\overline{MS}}^{(4)}$ is fitted to the corrected data considering statistical correlation between bins
- the fit result is:
  $\alpha_S(M_Z) =$
  $0.118 \pm 0.002(stat)^{+0.007}_{-0.008}(syst)^{+0.007}_{-0.006}(theo)$
  corresponding to $\Lambda_{\overline{MS}}^{(4)} = 320 \pm 33$ MeV
- QCD in NLO and corrected data agree for α_S^{fit}
- largest uncertainties due to:
  - the model dependence (LEPTO, ARIADNE, HERWIG...)
  - the parton densities
  - the renormalisation scale ambiguity ($\mu_R^2 = Q^2 \rightarrow 1/4$ and $4Q^2$)

DIS Event Shapes in the Breit Frame

- Phase Space in the Current Hemisphere of the Breit Frame for $e\,p \to e\,X$ Events:

$$Q/2$$

- Phase Space in one Hemisphere of $e^+e^- \to q\,\bar{q}$ Events:

$$\sqrt{s}/2$$

$\Rightarrow$ **Is there a relation between $e\,p$ Scattering and e^+e^- Annihilation concerning Event Shapes at a Scale:**

$$Q_{DIS} = \sqrt{s_{ee}}\ ?$$

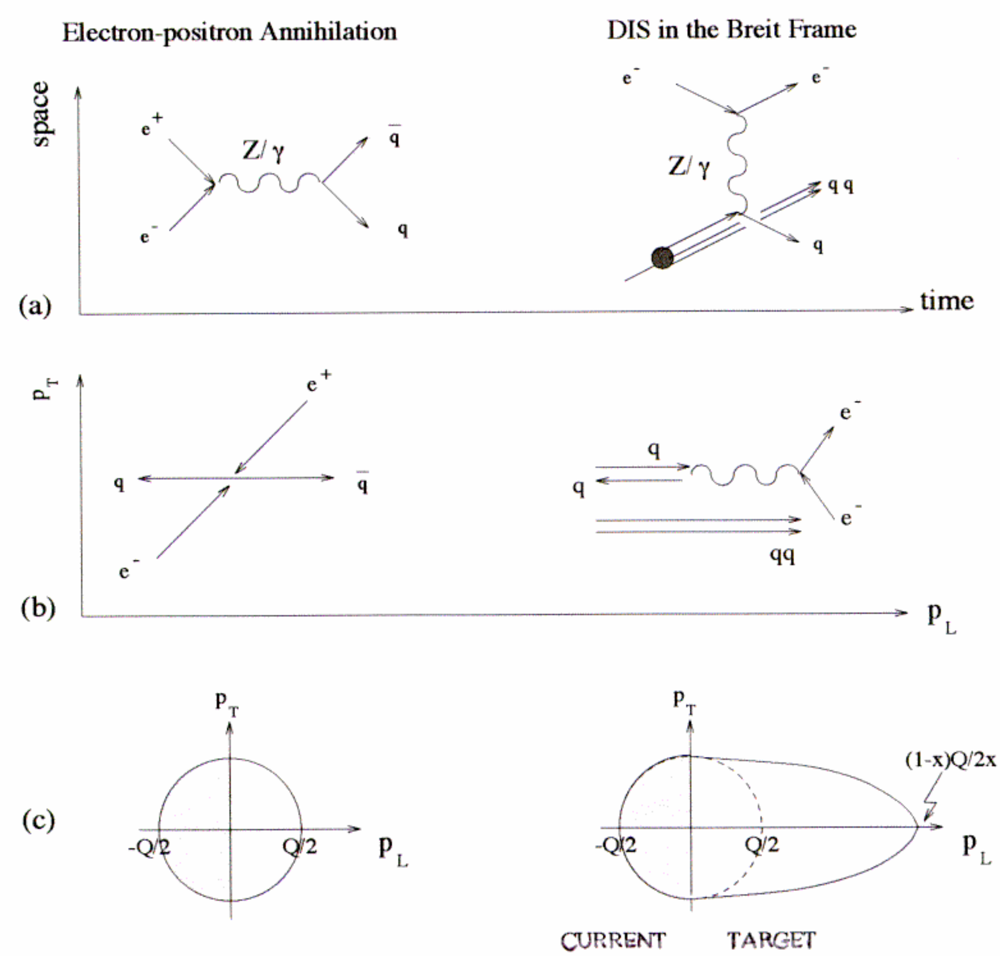

Power Corrections and $\alpha_s(M_Z)$

- Q or energy dependence of event shape variables
  - (i) change of strong coupling constant $\alpha_s(Q) \propto 1/\ln(Q/\Lambda)$
  - (ii) power or so-called 'hadronisation' corrections $\propto 1/Q$

- Mean value of any infrared safe event shape variable $\langle F \rangle$
  (e.g. $F = 1 - T_c,\ (1 - T_z)/2,\ B_c,\ \rho_c$)
  can be written in DIS ep and in e^+e^- annihilation as:

$$\langle F \rangle = \langle F \rangle^{\text{pert}} + \langle F \rangle^{\text{pow}}$$

  – Perturbative part:

$$\langle F \rangle^{\text{pert}} = c_1\, \alpha_s(Q) + c_2\, \alpha_s^2(\mu_R)$$

  → coefficients c_1, c_2 from $\mathcal{O}(\alpha_s^2)$ DISENT calculations

  – Power corrections:

$$\langle F \rangle^{\text{pow}} = a_F \frac{16}{3\pi} \frac{\mu_I}{Q} \ln^p \frac{Q}{\mu_I} \left[\bar{\alpha}_0(\mu_I) - \alpha_s(Q) - \frac{\beta_0}{2\pi} \left(\ln \frac{Q}{\mu_I} + \frac{K}{\beta_0} + 1 \right) \alpha_s^2(Q) \right]$$

Dokshitzer,Webber: $1/Q$ corrections not necessarily related to hadronisation. Power corrections may be due to a "universal" soft gluon phenomenon associated with the behaviour of the running coupling at small momentum scales. "Universal" means that they could be expressible in terms of a few non-perturbative parameters with calculable process dependent coefficients a_F and p.

→ contain a non-perturbative parameter $\bar{\alpha}_0(\mu_I)$
to be evaluated at some 'infrared matching' scale: $\Lambda \ll \mu_I \ll Q$

- QCD Analysis of $\langle F \rangle$ → $\bar{\alpha}_0$ and $\alpha_s(M_Z)$
  - **Power corrections $\propto 1/Q$ for all $\langle F \rangle$**
  - **Universal power correction parameters $\bar{\alpha}_0$ for all $\langle F \rangle$**

Event Shape Variables in the Breit Current Hemisphere

- **Thrust T_c**

$$T_c = \max \frac{\sum_h |\mathbf{p}_h \cdot \mathbf{n}_T|}{\sum_h |\mathbf{p}_h|} \qquad \mathbf{n}_T \equiv \text{thrust axis}$$

- **Thrust T_z** closer to $e^+ e^-$ annihilation

$$T_z = \frac{\sum_h |\mathbf{p}_h \cdot \mathbf{n}|}{\sum_h |\mathbf{p}_h|} = \frac{\sum_h |\mathbf{p}_{z\,h}|}{\sum_h |\mathbf{p}_h|} \qquad \mathbf{n} \equiv \text{hemisphere axis}$$

- **Jet Broadening B_c**

$$B_c = \frac{\sum_h |\mathbf{p}_h \times \mathbf{n}|}{2 \sum_h |\mathbf{p}_h|} = \frac{\sum_h |\mathbf{p}_{\perp\,h}|}{2 \sum_h |\mathbf{p}_h|} \qquad \mathbf{n} \equiv \text{hemisphere axis}$$

- **Jet Mass ρ_c**

$$\rho_c = \frac{M^2}{Q^2} = \frac{(\sum_h p_h)^2}{Q^2}$$

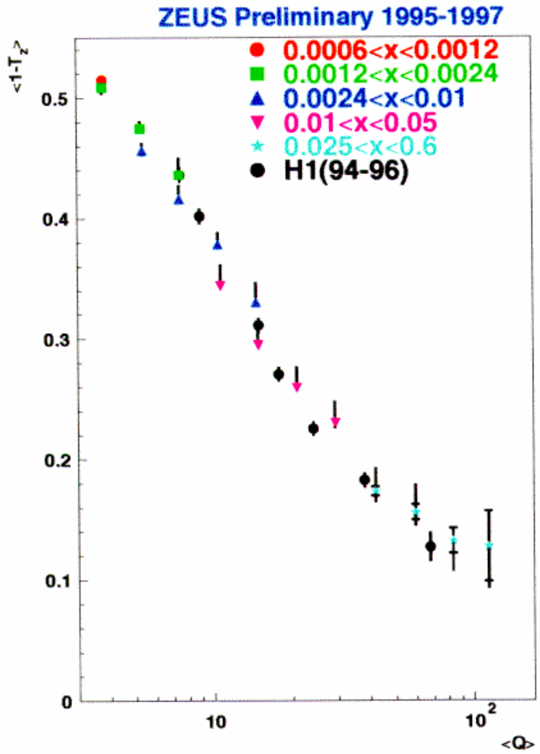

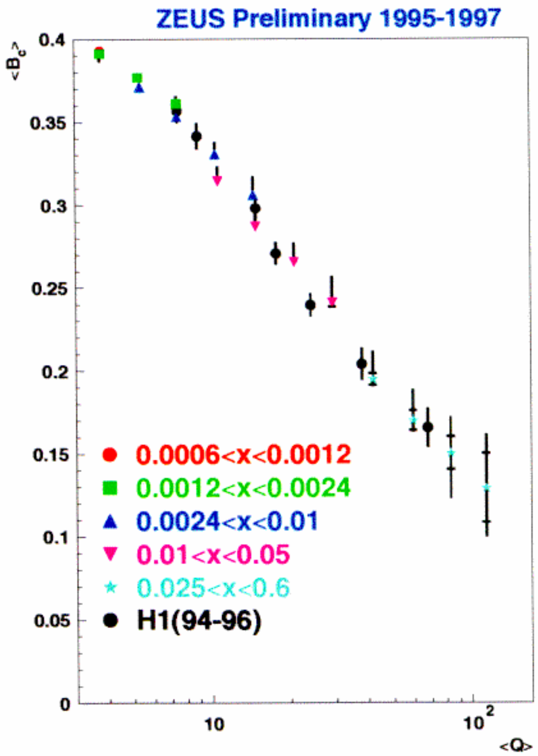

Results of QCD fits and Conclusions

Observable	$\bar{\alpha}_0(\mu_I = 2\ \text{GeV})$	$\alpha_s(M_Z)$	χ^2/ndf
H1 ep data			
$\langle 1-T_c \rangle$	$0.481 \pm 0.005\ ^{+0.109}_{-0.036}$	$0.123 \pm 0.002\ ^{+0.007}_{-0.005}$	5.1/5
$\langle 1-T_z \rangle / 2$	$0.492 \pm 0.010\ ^{+0.109}_{-0.051}$	$0.115 \pm 0.002\ ^{+0.007}_{-0.005}$	8.1/5
$\langle B_c \rangle$	$0.375 \pm 0.008\ ^{+0.036}_{-0.022}$	$0.116 \pm 0.002\ ^{+0.007}_{-0.004}$	5.3/5
$\langle \rho_c \rangle$	$0.454 \pm 0.009\ ^{+0.025}_{-0.020}$	$0.130 \pm 0.003\ ^{+0.007}_{-0.005}$	2.8/5
common fit			
$T_c + T_z + \rho_c$	**$0.491 \pm 0.003\ ^{+0.079}_{-0.042}$**	**$0.118 \pm 0.001\ ^{+0.007}_{-0.006}$**	39/19
e^+e^- data			
$\langle 1-T_{ee} \rangle$	$0.519 \pm 0.009\ ^{+0.093}_{-0.039}$	$0.123 \pm 0.001\ ^{+0.007}_{-0.004}$	10.9/14
$\langle M_H^2/s \rangle$	$0.580 \pm 0.015\ ^{+0.130}_{-0.053}$	$0.119 \pm 0.001\ ^{+0.004}_{-0.003}$	10.9/14

- First Analysis at HERA of the DIS Event Shape Parameters $1-T_C,\ 1-T_Z,\ B_C,\ \rho_C$ in the Breit Current Hemisphere with the coverage of a large range in $Q = 7 \div 100$ GeV in a Single Experiment
- The Event Shapes become more collimated with rising Q as expected. and give consistent results. They are compatible with a Universal Power Correction Parameter $\bar{\alpha}_0 \approx 0.5$ within $\pm 20\,\%$.
- The Strong Coupling Constant $\alpha_s(M_Z)$ and $\bar{\alpha}_0$ are simultaneously determined independently of Fragmentation Models using $\mathcal{O}(\alpha_s^2)$ Calculations of DISENT and MEPJET.
- The comparison with e^+e^- Experiments shows that the Q Dependence of Thrust and Jet Masses is in gross agreement despite differences in the underlying Physics and the analysis methods. The same Power Correction Parameters $\bar{\alpha}_0$ are found within $\pm 20\,\%$ of ep results.

Summary of α_S determinations from Hadronic final states at HERA

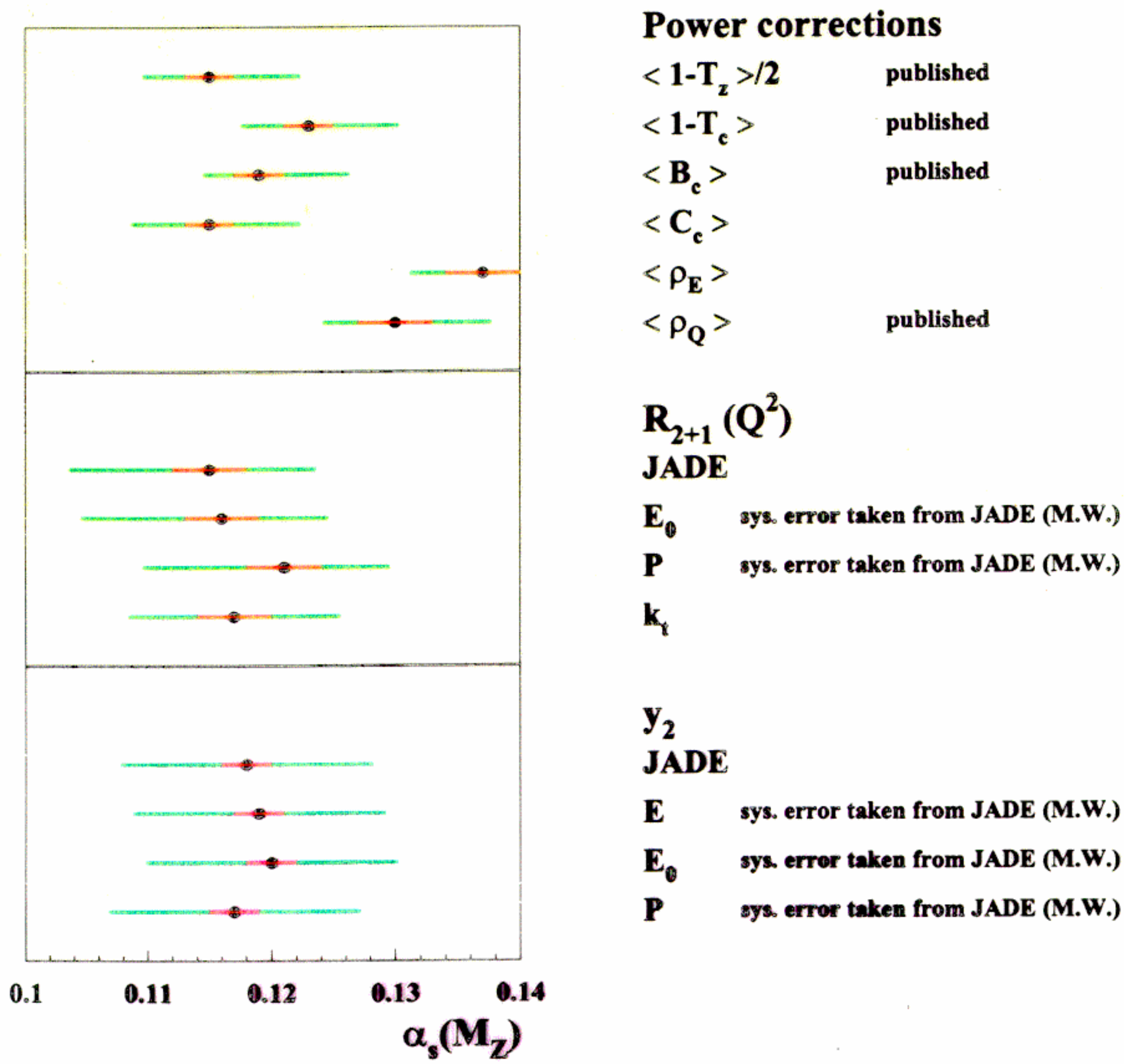

- impressive progress in study of hadronic final states:

  largely increased data samples; improved NLO programs; improved MC models; many new analyses

- many open questions are waiting to be answered and further improvement is to be expected

DIS Events at High Q^2

High Q^2 Neutral Current (NC)

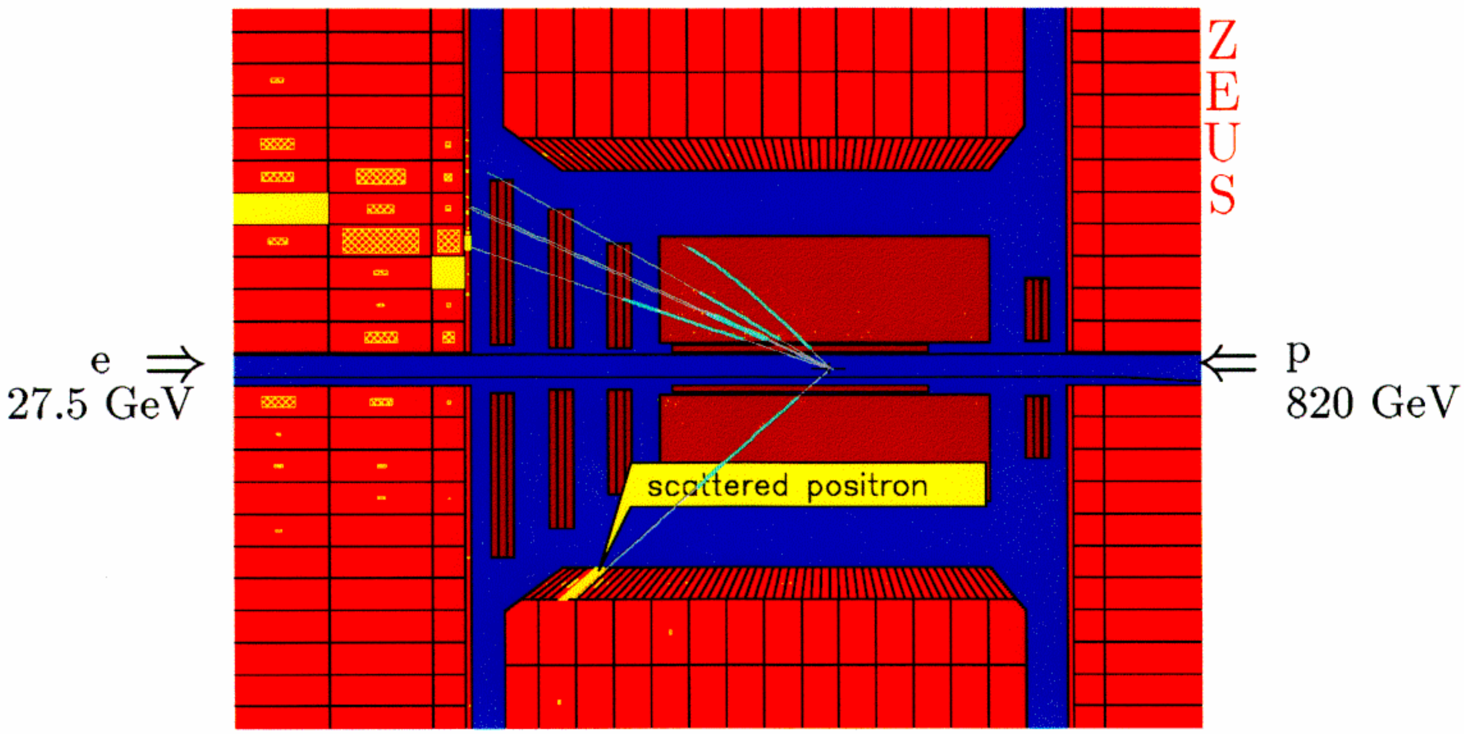

High Q^2 Charged Current (CC)

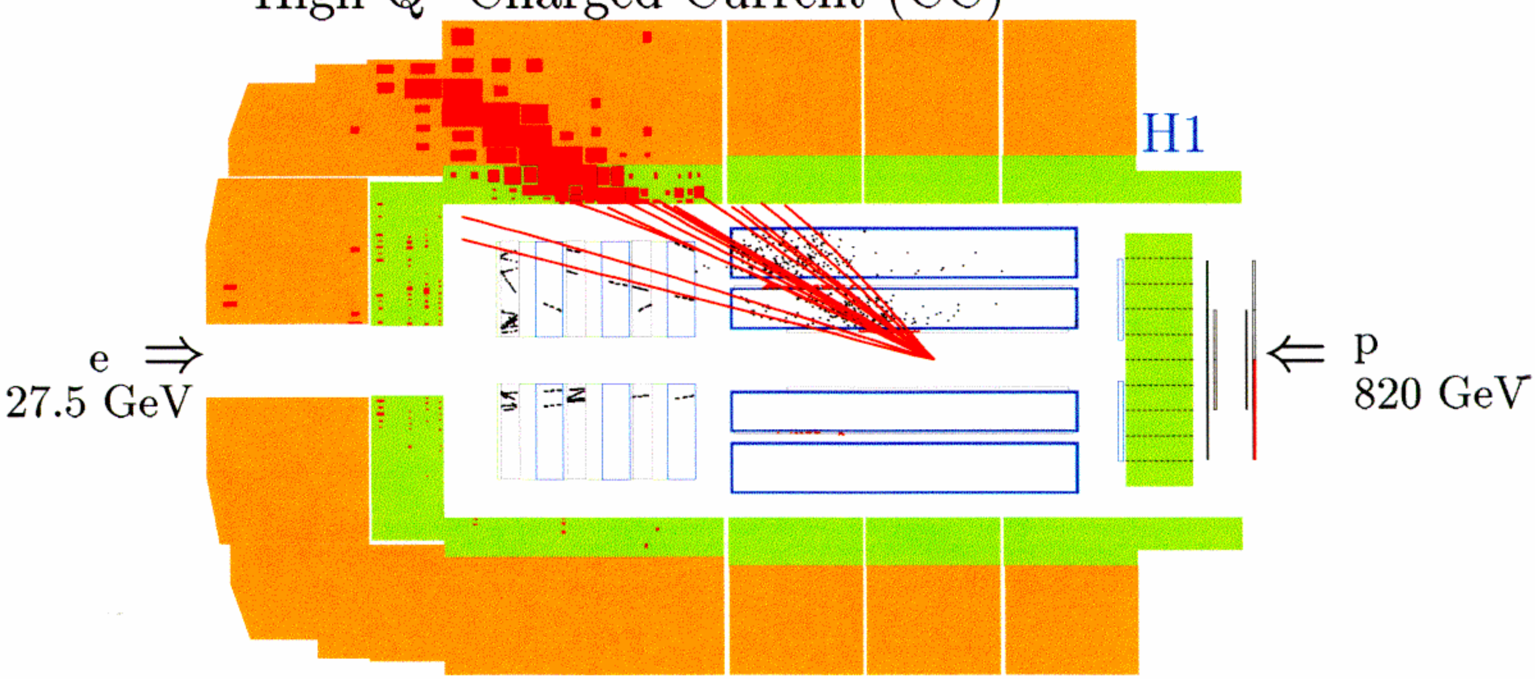

Electron Energy Calibration

- **In situ** e.m. calibration of the LAr calorimeter using :

  Double-angle method and ω-method for NC DIS
  Double-angle method and P_T balance for QED Comptons

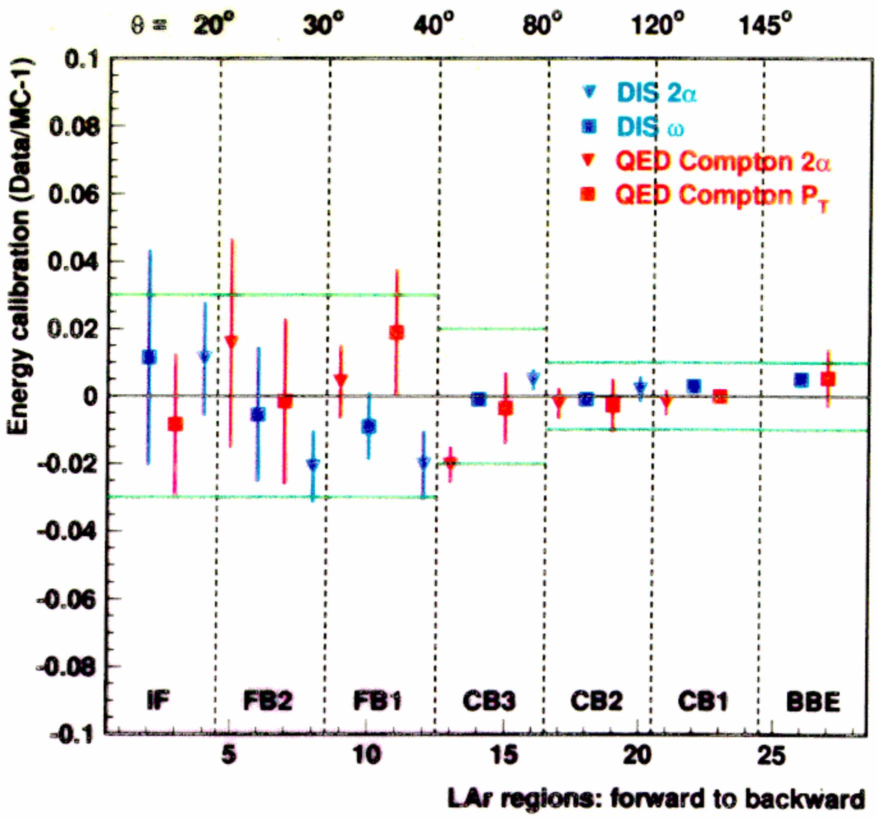

- Backward LAr wheels:
  ⇒ 1% precision for θ between 80° to 150°
- Forward LAr wheels:
  Consistency from various methods
  using NC DIS and QED Comptons
  ⇒ Calibration scale improved.
  ⇒ 3% uncertainty only limited by statistics

Hadronic Energies

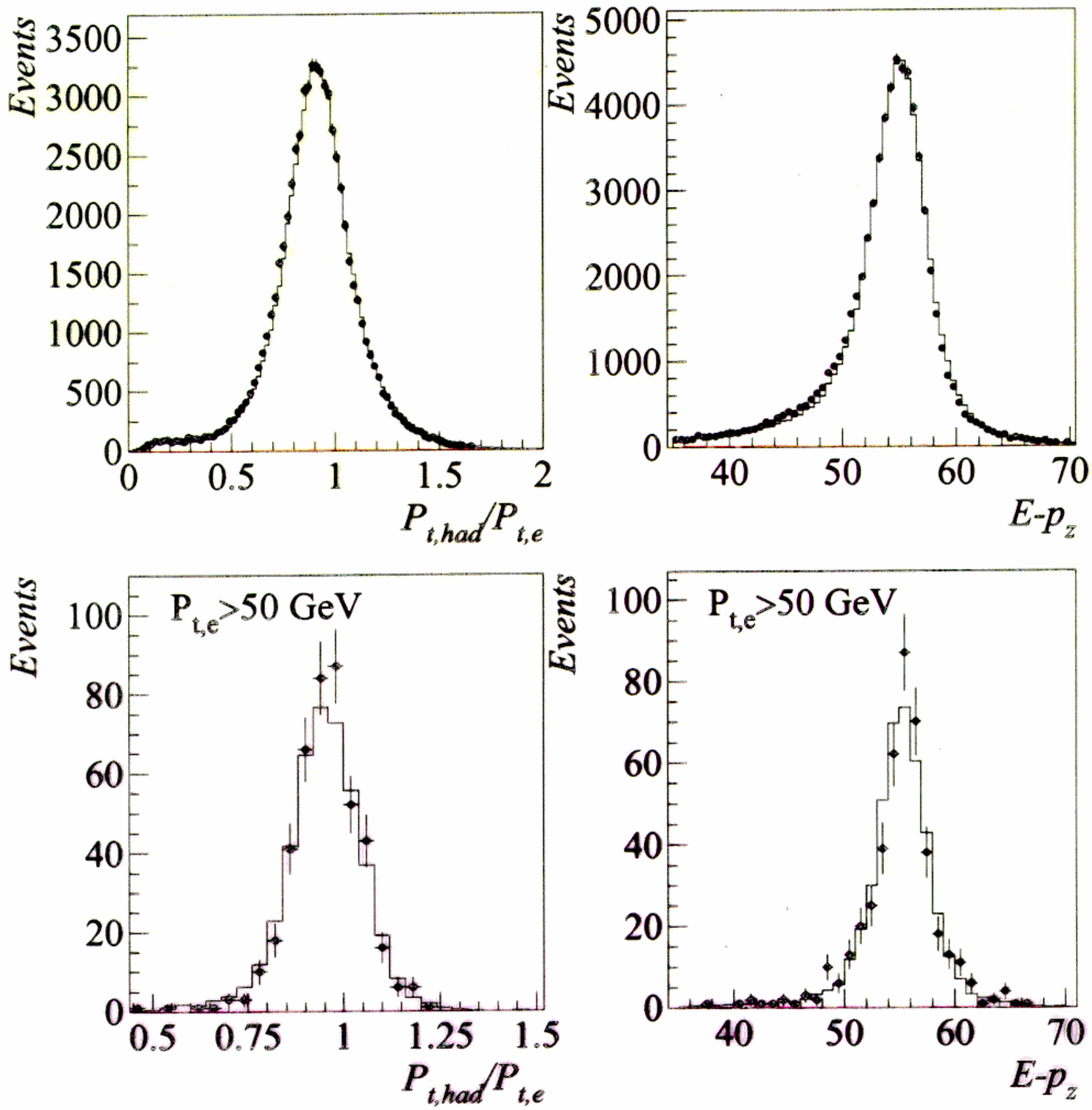

- Hadronic scale is being precisely calibrated using the electron as reference
- Width and scale of the hadronic distributions well described at low and high P_T

$\mathbf{d}\boldsymbol{\sigma}/\mathbf{d}\boldsymbol{x}$ at $\boldsymbol{Q}^2 > \mathbf{1000}, \mathbf{10000}$ GeV^2

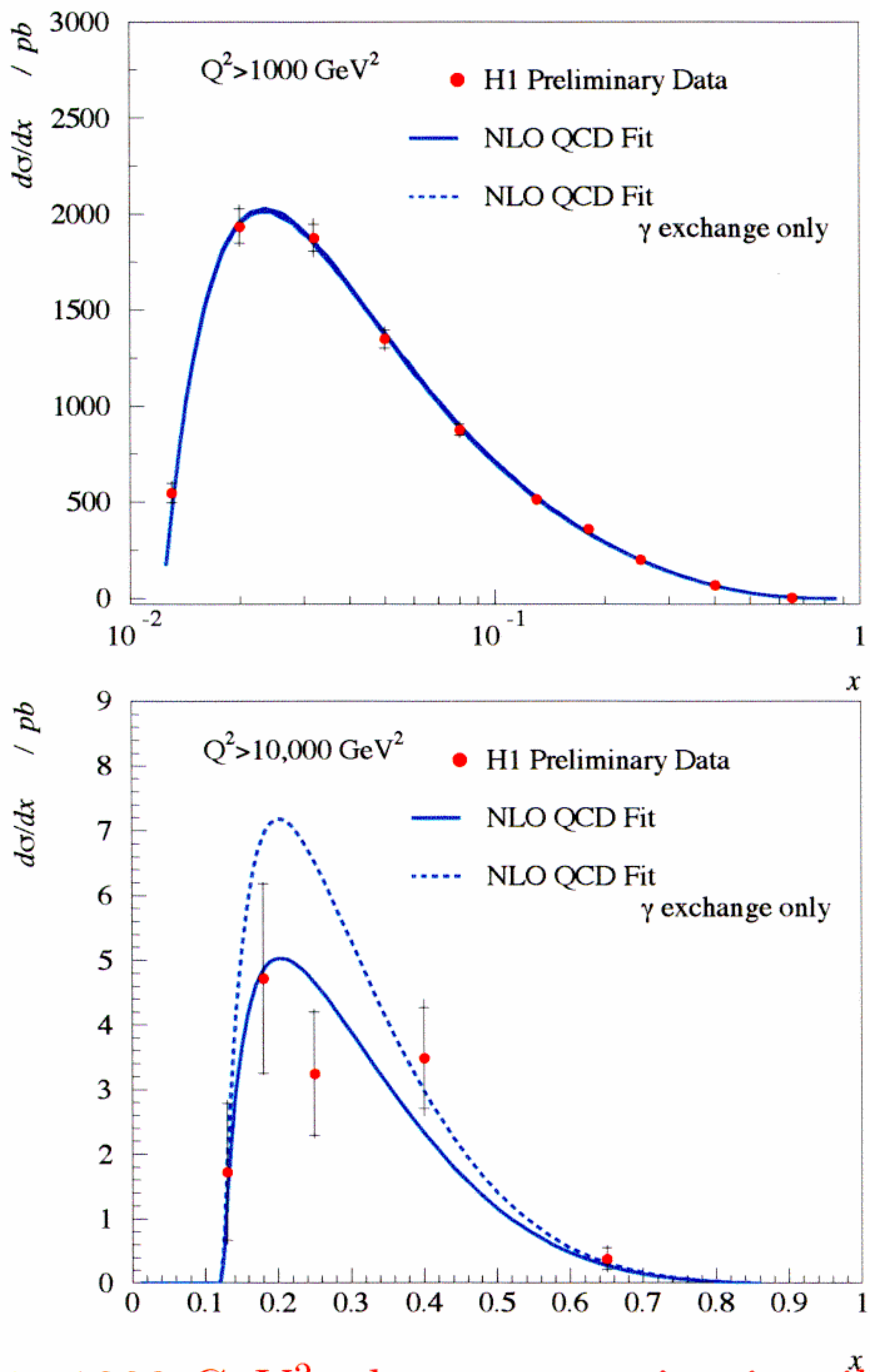

- For $Q^2 \geq 1000$ GeV^2, the cross-section is still dominated by low x parton scattering.
- For $Q^2 \geq 10000$ GeV^2 the valence quarks contribute.
- The data are in good agreement with the electroweak Standard Model. Z exchange needed!

Neutral Current Cross-Sections

Kinematic Domain: $200\ \mathrm{GeV}^2 \leq Q^2 \leq 30000\ \mathrm{GeV}^2$
$0.005 \leq x \leq 0.65$

$$\frac{d^2\sigma^{e^+p}}{dx\,dQ^2} = \frac{2\pi\alpha^2}{xQ^4}\left[Y_+F_2(x,Q^2) - y^2F_L(x,Q^2) - Y_-xF_3(x,Q^2)\right]$$

$$Y_\pm(y) = 1 \pm (1-y)^2$$

F_2,F_3: generalized structure functions
F_L: longitudinal structure function

$$F_2 = F_2^{em} + \frac{Q^2}{(Q^2+M_Z^2)}F_2^{int} + \frac{Q^4}{(Q^2+M_Z^2)^2}F_2^{wk} = F_2^{em}(1+\delta_Z)$$

F_2^{em}: photon exchange
F_2^{wk}: Z° exchange
F_2^{int}: γZ° interference

In the following we will use the Reduced Cross-Section:

$$\tilde{\sigma}(e^+p) \equiv \frac{xQ^4}{2\pi\alpha^2}\frac{1}{Y_+}\frac{\mathrm{d}^2\sigma}{\mathrm{d}x\mathrm{d}Q^2}$$
$$\approx F_2^{em}(1+\delta_Z-\delta_3-\delta_L)$$

$\delta_Z - \delta_3$: $< 1\%$ at $Q^2 < 1500\ \mathrm{GeV}^2$
$\approx 10\%$ at $Q^2 = 5000\ \mathrm{GeV}^2$ and x=0.08

δ_L: negligible at $y < 0.5$
$\approx 5\%$ at $y = 0.9$

Contributions to the NC Cross-Section

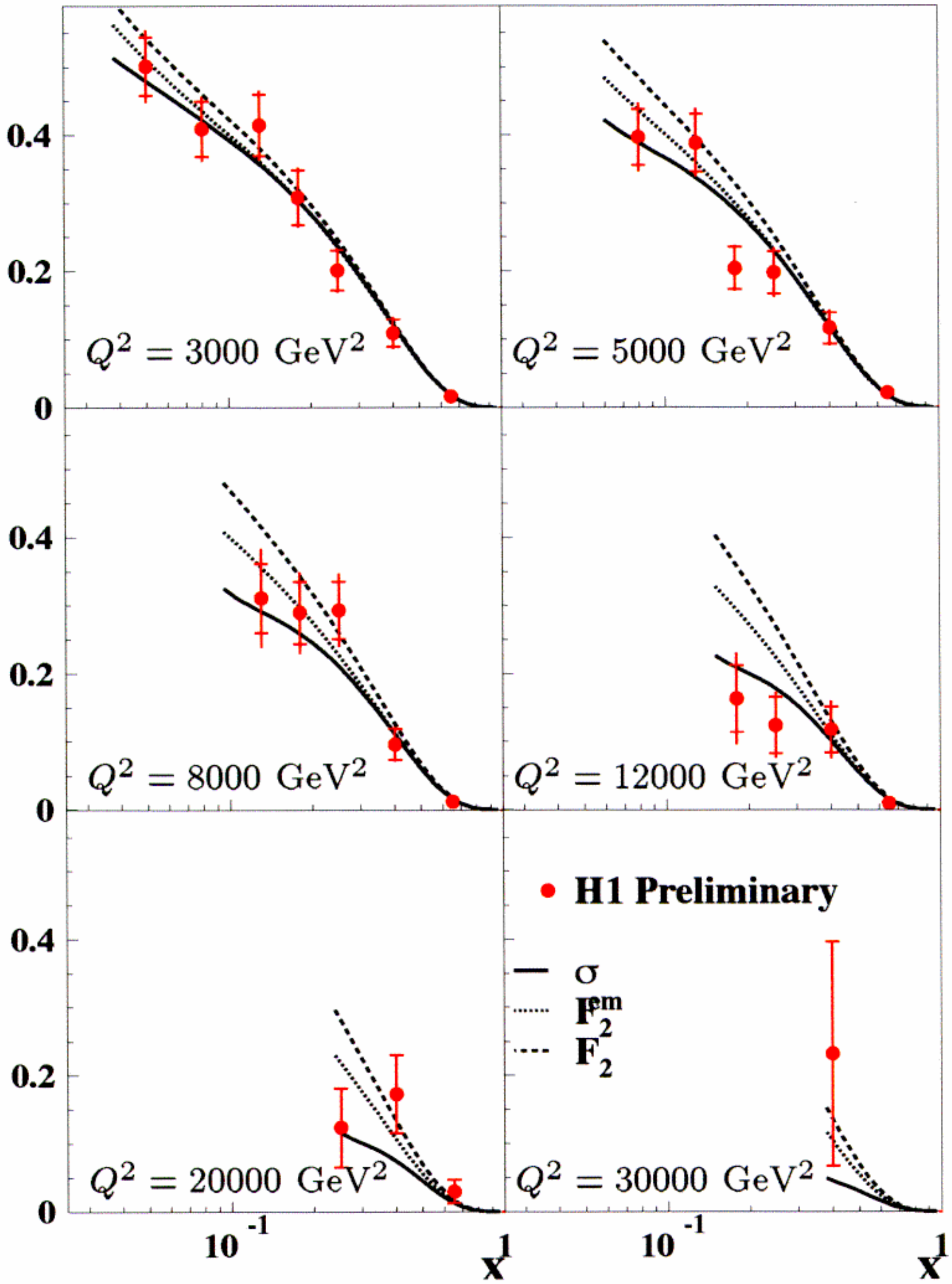

⇒ at $Q^2 \geq 15000$ GeV^2
no structure function
has a dominant contribution!

Reduced Neutral Current Cross-Section

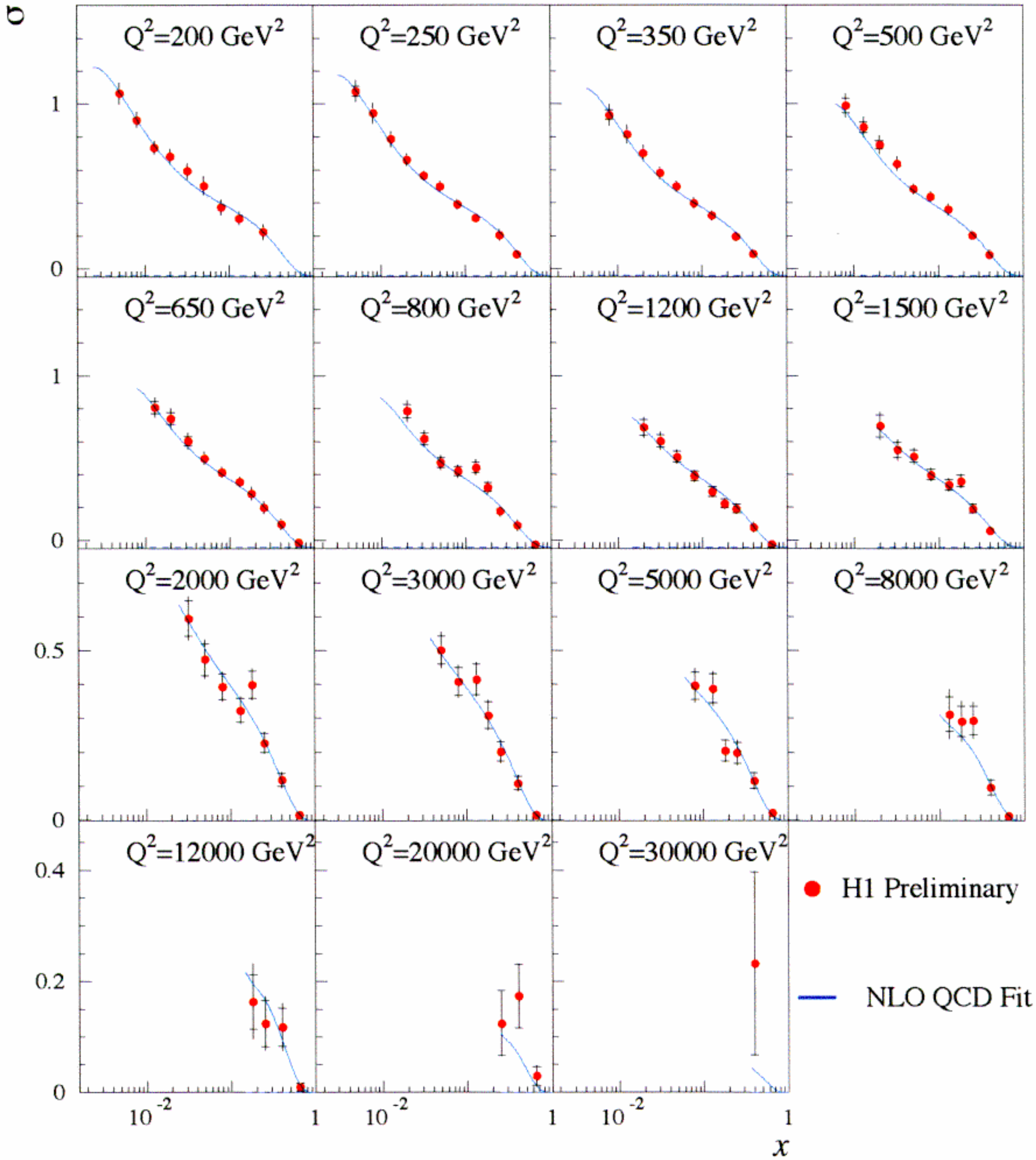

- Measurement from $Q^2 = 200$ to $30000\ \mathrm{GeV}^2$, up to $x = 0.65$ for $Q^2 \geq 650\ \mathrm{GeV}^2$.
- NLO QCD fit gives good description of the data in the whole Q^2 and x range
- Precision limited by statistics at $Q^2 > 1000\ \mathrm{GeV}^2$
- total error (syst $\oplus$ stat) $< 10\%$ except at high Q^2

Reduced Cross-Section at High x

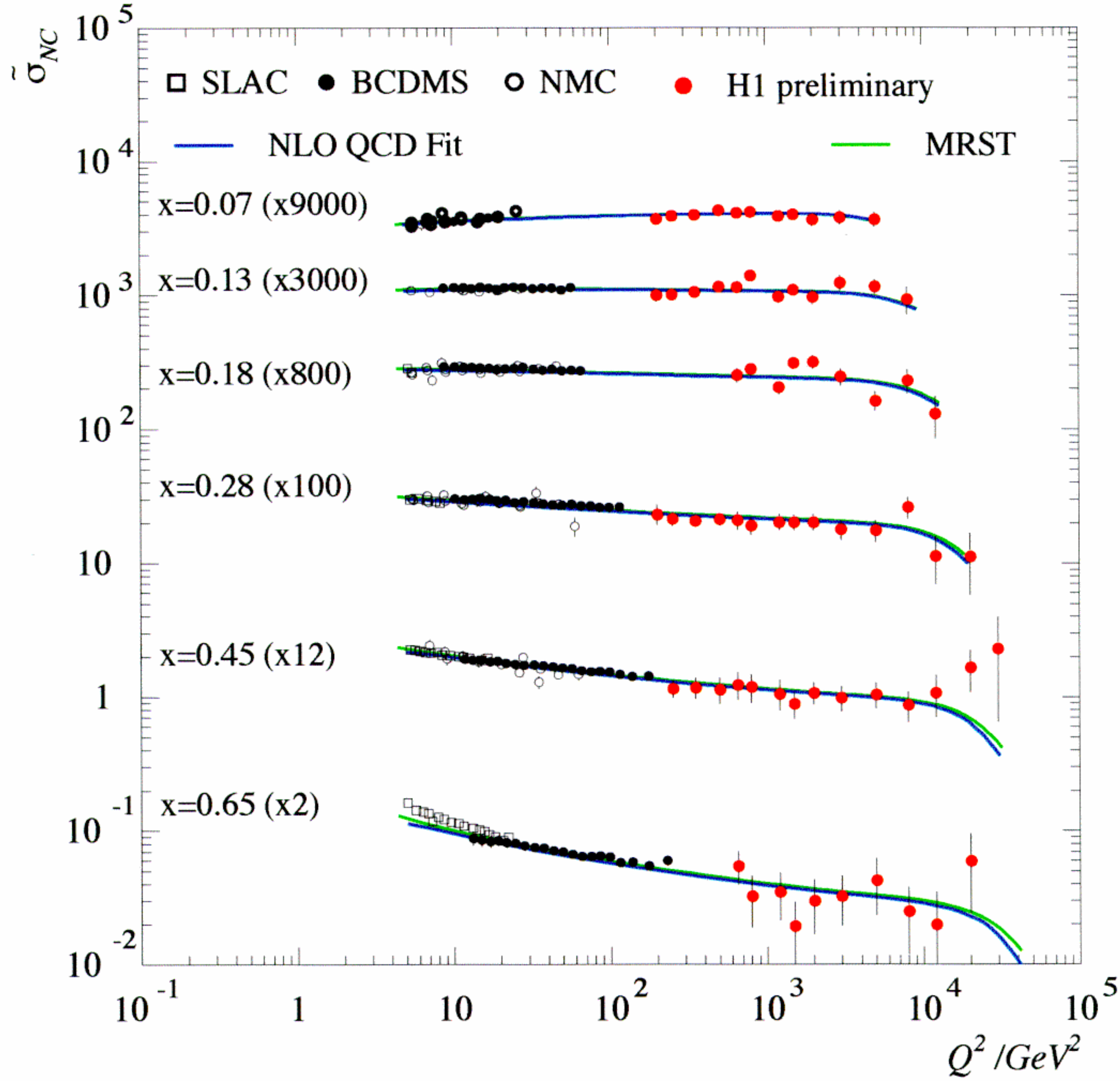

- Difference visible in the QCD fit when the high Q^2 data is or is not included.
- High Q^2 HERA data now also have an influence at **high** x ($\approx 5\%$ **at highest** Q^2).
- α_S measurement from $dF_2/d\ln Q^2$ at high x in future.

Charged Current Cross-Sections

Cross Section for $e^+p \longrightarrow \bar{\nu}X$:

$$\frac{d^2\sigma}{dxdQ^2} = \frac{G_F^2}{2\pi}\frac{1}{(1+Q^2/M_W^2)^2}\left(\bar{u}+\bar{c}+(1-y)^2(d+s)\right)$$

- Propagator dependence ⇒ W mass determination

  H1 (94-97): $81.2 \pm 3.3 \pm 4.3$ GeV

  ZEUS (94-97): $78.6^{+2.5+3.3}_{-2.4-3.0}$ GeV

- parton densities ⇒ sensitivity to d-quark density
- helicity dependence ⇒ V-A coupling
- QED radiative Corrections ($< 10\%$) applied

Reduced Charged Current Cross-Section:

$$\sigma_{CC} \equiv x \cdot \frac{2\pi}{G_F^2}(1+Q^2/M_W^2)^2\frac{d^2\sigma}{dxdQ^2}$$
$$= x \cdot \left(\bar{u}+\bar{c}+(1-y)^2(d+s)\right) \textit{ in QPM}$$

- definition in analogy to the Reduced Neutral Current Cross-Section
- different relation to the parton densities: supression of the valence quark contribution at high y due to the helicity factor

The propagator Mass M_W

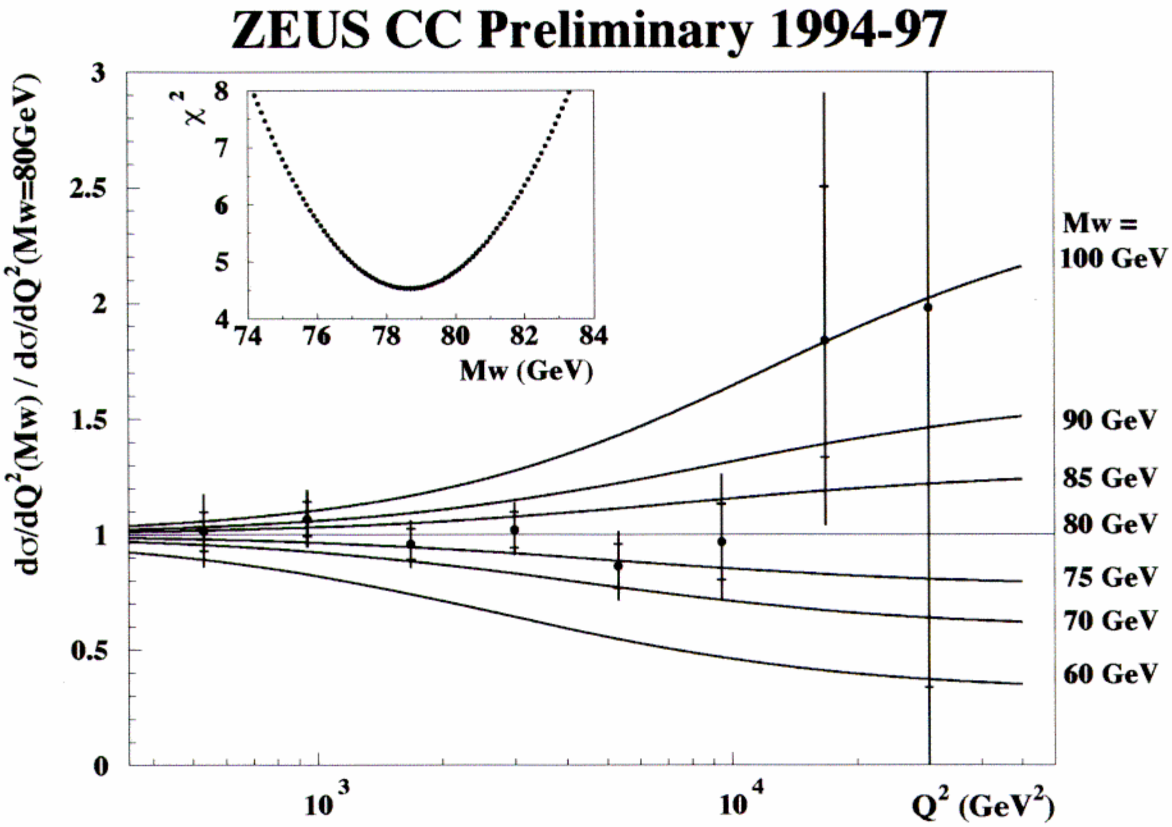

- The Q^2 dependence of the CC cross-section is determined by the propagator mass (and the parton densities).

  ep : space-like measurement of M_W

  – $e^+e^-, p\bar{p}$: time-like measurement of M_W

$$\frac{d^2\sigma_{CC}}{dxdQ^2} = \frac{G_F^2}{2\pi x} \cdot \left(\frac{M_W^2}{M_W^2 + Q^2}\right)^2 \cdot \phi_{CC}(x, Q^2)$$

- input parameters: $\alpha, M_W, M_Z, M_{top}, M_H$
- parton densities: MRST (H1)/ CTEQ4D (ZEUS)

  H1 (94-97): $81.2 \pm 3.3 \pm 4.3$ GeV

  ZEUS (94-97): $78.6^{+2.5+3.3}_{-2.4-3.0}$ GeV

- in agreement with $M_W = 80.41 \pm 0.10$ GeV from pdg

CC reduced Cross-Section

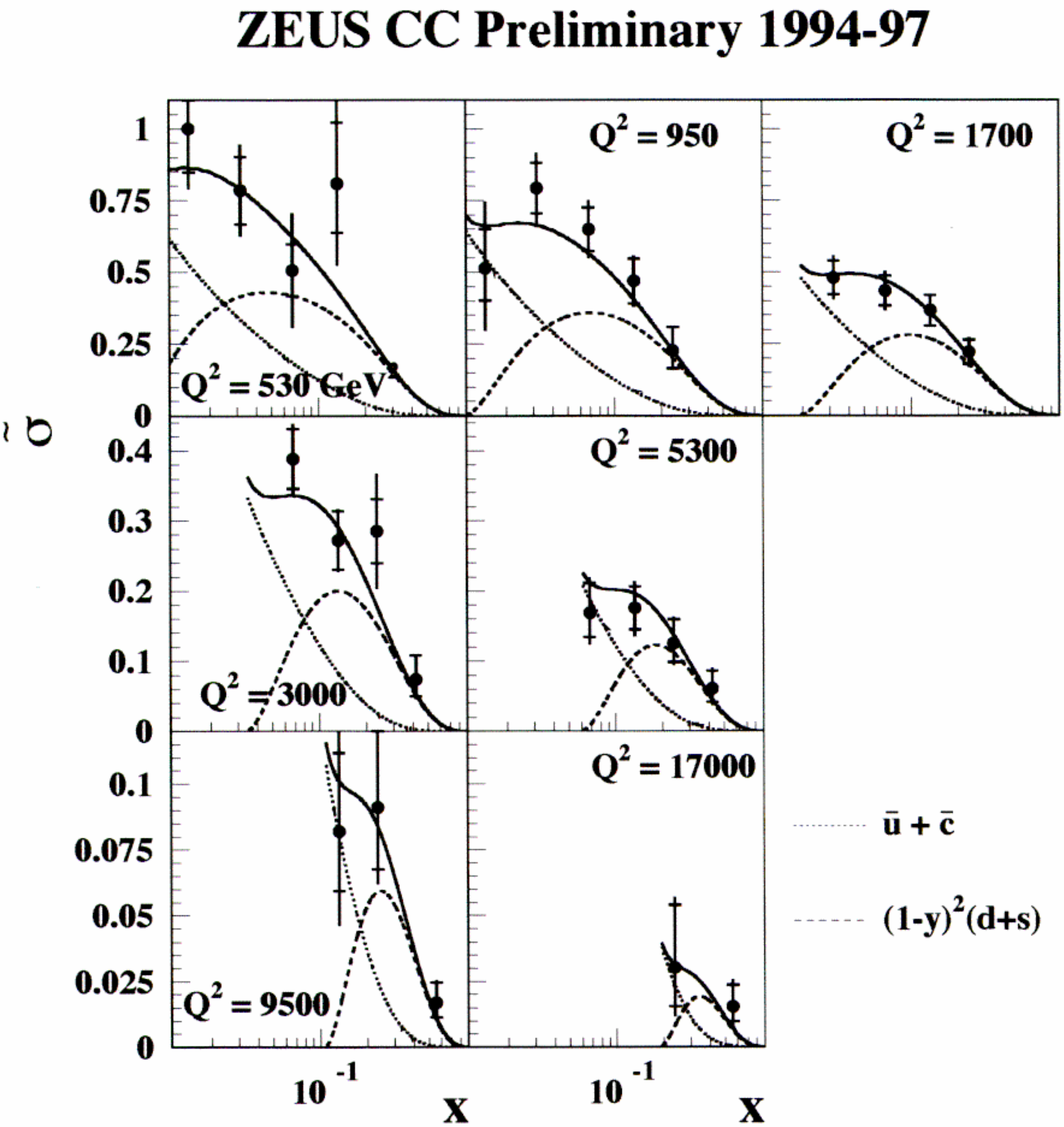

- Standard Model gives a good description of the CC cross-section
- d valence dominates at high x
- sea quarks dominate at low x

Can we measure the u/d ratio?

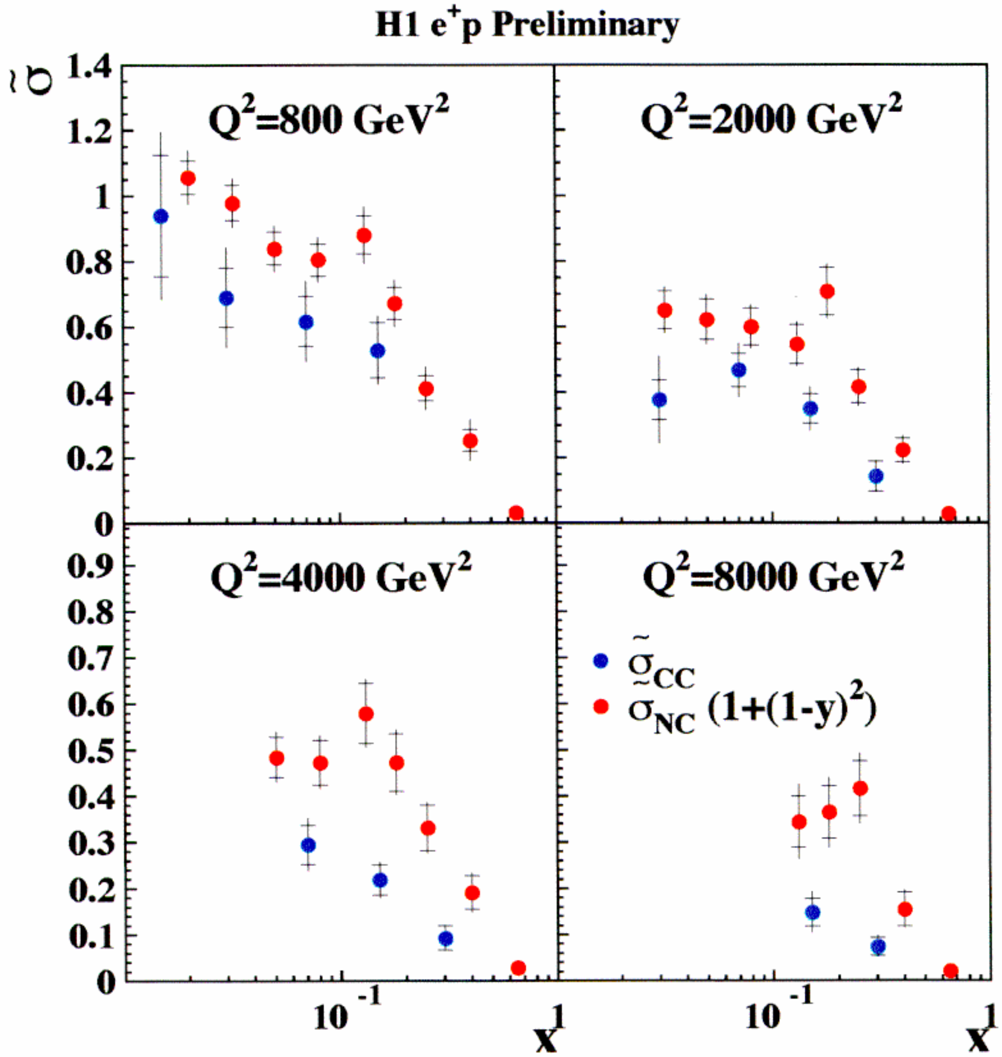

- neglecting xF_3, the S. F. term in L.O corresponds to:

$$1 + (1-y)^2 \left(\tfrac{4}{9}u + \tfrac{1}{9}d\right) \quad \text{in NC}$$

$$(1-y)^2 d \quad \text{in CC}$$

at 2000 GeV^2:

$$- \quad 0.83 \left(u + \tfrac{1}{4}d\right) \quad \text{in NC}$$

$$- \quad 0.86 \quad d \quad \text{in CC}$$

$\Rightarrow$ **u/d** ~ 2

Neutral and Charged Current Cross-Section

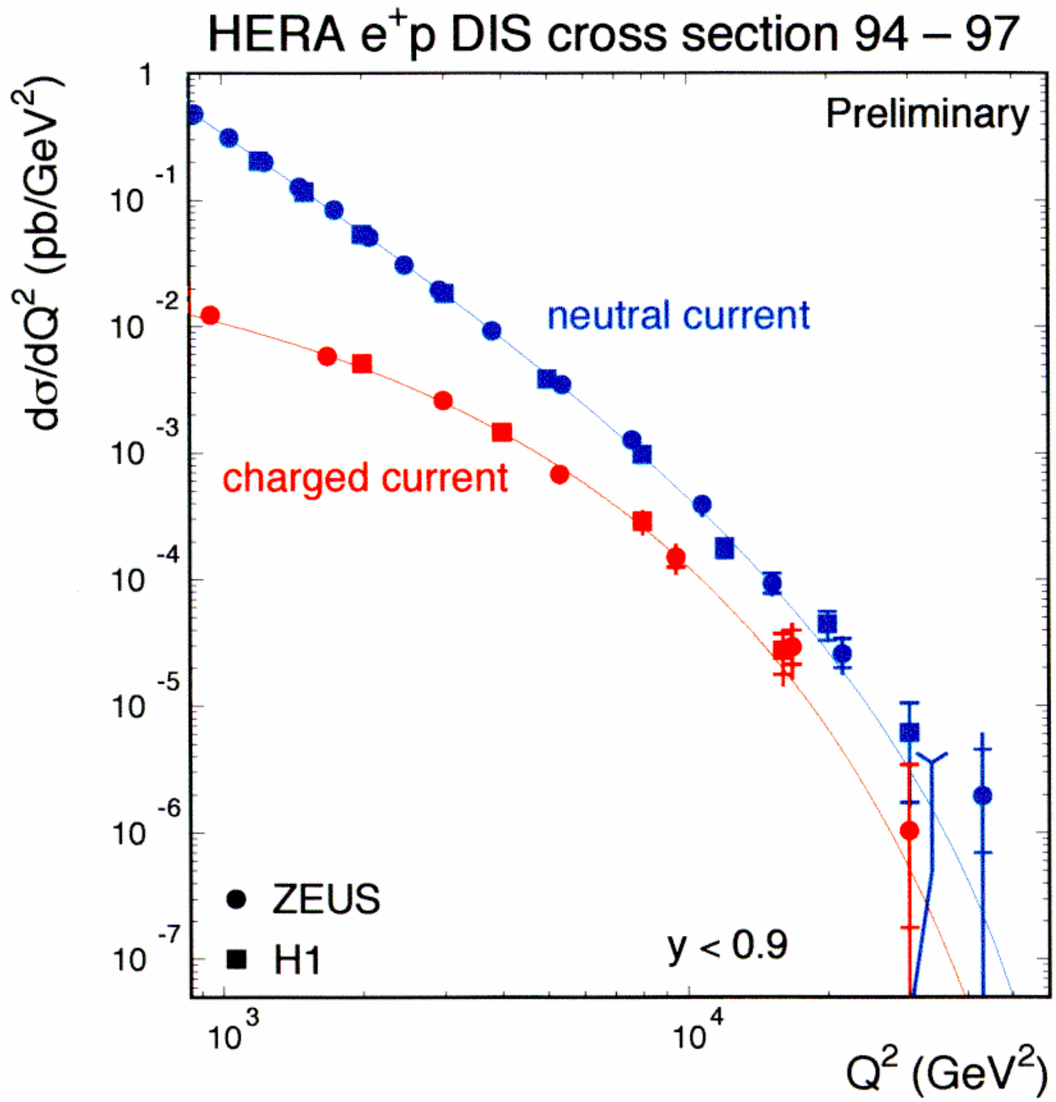

- Neutral and Charged Current Cross-Section have similar values at high Q^2
- remaining difference at high Q^2 are due to coupling to different quark flavours
- What happens at very high $Q^2 (\geq 15000 \text{ GeV}^2)$?

Summary

- In its first years of operation, HERA has been testing the SM, in particular QCD and the Proton Structure, in new kinematic domains.
- More is coming with the expected 50 pb^{-1} of e^-p data in 98-99 which will complement the e^+p results presented here:

  ⇒ α_S, xg, p.d.f. measured precisely
  ⇒ hadronic final state studied in detail
  ⇒ check the excess at high Q^2 in e^-p

  But also afterwards with the luminosity upgrade of HERA and its detectors in 2000. Between 2000 and 2005, 500-1000 pb^{-1} are expected.

  Program will continue with higher precision and with an extended search potential

Surprises?

see U. Katz talk!!!